Neuron
Article

SynCAM 1 Adhesion Dynamically Regulates Synapse Number and Impacts Plasticity and Learning

Elissa M. Robbins,[1,6] Alexander J. Krupp,[2,6] Karen Perez de Arce,[1] Ananda K. Ghosh,[1,4] Adam I. Fogel,[1,5] Antony Boucard,[3] Thomas C. Südhof,[3] Valentin Stein,[2,7] and Thomas Biederer[1,7,*]
[1]Department of Molecular Biophysics and Biochemistry, Yale University, New Haven, CT 06520, USA
[2]Max Planck Institute of Neurobiology, 82152 Martinsried, Germany
[3]Department of Molecular and Cellular Physiology, Stanford University, Palo Alto, CA 94304, USA
[4]Present address: Department of Pharmacology, Cornell University, New York, New York 10021, USA
[5]Present address: National Institute of Neurological Disorders and Stroke, Bethesda, Maryland 20892, USA
[6]These authors contributed equally to this work
[7]These authors contributed equally to this work
*Correspondence: thomas.biederer@yale.edu
DOI 10.1016/j.neuron.2010.11.003

SUMMARY

Synaptogenesis is required for wiring neuronal circuits in the developing brain and continues to remodel adult networks. However, the molecules organizing synapse development and maintenance in vivo remain incompletely understood. We now demonstrate that the immunoglobulin adhesion molecule SynCAM 1 dynamically alters synapse number and plasticity. Overexpression of SynCAM 1 in transgenic mice promotes excitatory synapse number, while loss of SynCAM 1 results in fewer excitatory synapses. By turning off SynCAM 1 overexpression in transgenic brains, we show that it maintains the newly induced synapses. SynCAM 1 also functions at mature synapses to alter their plasticity by regulating long-term depression. Consistent with these effects on neuronal connectivity, SynCAM 1 expression affects spatial learning, with knock-out mice learning better. The reciprocal effects of increased SynCAM 1 expression and loss reveal that this adhesion molecule contributes to the regulation of synapse number and plasticity, and impacts how neuronal networks undergo activity-dependent changes.

INTRODUCTION

Synapse formation is required for the development of the nervous system and dynamic changes of synapses in the mature brain are associated with cognitive functions such as learning and memory. Notably, aberrant synapse structures are present in mental retardation and neurological disorders (Fiala et al., 2002; Irwin et al., 2001). Elucidating the molecular machinery that organizes synapses is therefore relevant to our understanding both of physiological functions as well as debilitating brain disorders.

Protein interactions across the synaptic cleft are now known to organize developing synapses (Biederer and Stagi, 2008; Giagtzoglou et al., 2009; Jin and Garner, 2008). Postsynaptic adhesion molecules of the neuroligin and SynCAM families and EphB receptors drive the differentiation of synapses (Biederer et al., 2002; Chih et al., 2005; Chubykin et al., 2007; Graf et al., 2004; Kayser et al., 2006; Nam and Chen, 2005; Scheiffele et al., 2000). In addition, neuroligins control synapse specification and maturation (Chubykin et al., 2007; Varoqueaux et al., 2006), while cadherins contribute to the structural development and plasticity of synapses (Okamura et al., 2004; Togashi et al., 2002). Mutations in neuroligin and neurexin genes have been linked to familial forms of autism-spectrum disorders, supporting the hypothesis that synapse disorganization and imbalanced neuronal excitation can result in neurodevelopmental disorders (Bourgeron, 2009; Südhof, 2008; Zoghbi, 2003). Consistent with the physiological relevance of synapse-organizing molecules, links of SynCAM 1 and cadherins to autism-spectrum disorders have also been reported (Wang et al., 2009; Zhiling et al., 2008).

Among the select proteins that drive synapse formation, SynCAM 1 (also known as Cadm1 and nectin-like molecule 2) is the founding member of a family of four immunoglobulin (Ig) proteins that are expressed throughout the developing and mature brain (Biederer, 2006; Thomas et al., 2008). SynCAM 1 participates in axo-dendritic interactions, indicating early roles in the contact-mediated differentiation of synapses (Stagi et al., 2010). At later developmental stages, SynCAM proteins are enriched in pre- and postsynaptic plasma membranes and engage in specific homo- and heterophilic adhesive interactions (Biederer et al., 2002; Fogel et al., 2007). Functionally, the heterophilic partners SynCAM 1 and SynCAM 2 drive presynaptic terminal formation in cultured neurons and increase the number of excitatory, but not inhibitory synapses (Biederer et al., 2002; Fogel et al., 2007; Sara et al., 2005).

Despite the significant molecular insights into the synapse-organizing roles of *trans*-synaptic interactions, three decisive aspects remain insufficiently understood. First, to which extent are synapse numbers regulated by synaptic adhesion in the

brain? Second, at which steps during the lifetime of synapses are individual synaptic adhesion molecules engaged? Third, do these synapse-organizing proteins alter synaptic physiology and affect neuronal network functions?

We now demonstrate that SynCAM 1 significantly impacts these three aspects. Combining electron microscopy, Golgi staining, and electrophysiology, we demonstrate that elevated expression of SynCAM 1 in a transgenic mouse model increases functional excitatory synapse number. This activity corresponds to its endogenous role, as SynCAM 1 knock-out (KO) mice exhibit fewer excitatory synapses. Moreover, SynCAM 1 functions dynamically at developing synapses: Using the temporal control afforded by the design of our transgenic model, we show that continued SynCAM 1 elevation is required to maintain the increase in synapse number it drives in the first place. Unexpectedly, SynCAM 1 additionally alters the plasticity of synapses once they are formed, with its overexpression abrogating long-term depression (LTD) and its loss increasing LTD. These complementary changes in synapse number and plasticity correlate with altered cognitive functions and SynCAM 1 KO mice exhibit improved spatial learning. Our results reveal important contributions of SynCAM 1 to excitatory synapse number and function in the developing and adult brain. This supports a model that synaptic adhesion by SynCAM 1 can promote synapse formation and restrict synaptic plasticity to regulate the wiring and remodeling of neuronal circuits.

RESULTS

SynCAM Proteins Are Prominent in Synaptic Plasma Membranes

To gain better molecular insight into SynCAM properties in vivo, we determined the abundance of the four SynCAM family members. Quantitative immunoblotting of synaptic plasma membranes purified at postnatal day 9 (P9), when excitatory synapse formation begins to peak in the forebrain, showed that the heterophilic adhesion partners SynCAM 1 and 2 accounted for 0.41 ng/μg and 4.0 ng/μg of total synaptic membrane proteins, respectively. SynCAM 3 and 4 were present at 0.46 ng/μg and 0.20 ng/μg in this fraction. Thus, 0.5% of synaptic membrane proteins were comprised of SynCAM proteins at this developmental stage, a high fraction even when compared to the most abundant synaptic protein CaMKII that constitutes 7% of the postsynaptic density (Cheng et al., 2006). Correspondingly, SynCAM proteins were prominent in brain homogenates (see Table S1 available online) where they are considerably more abundant than neuroligins (Varoqueaux et al., 2006). This prominent expression indicated that SynCAM proteins could play important roles at synapses.

Overexpression of SynCAM 1 with Temporal Control

Redundancy and compensation between synapse-organizing proteins may preclude the identification of phenotypes in mice lacking single synaptic adhesion molecules as previously reported (Varoqueaux et al., 2006). Specifically, the single loss of SynCAM 1 in KO mice may be compensated by other SynCAM family members or functionally related proteins. We therefore reasoned that elevating SynCAM 1 in neurons may expose its in vivo activities more readily than a loss-of-function approach. To pursue the overexpression of SynCAM 1 in vivo, we generated a mouse line carrying a transgene encoding flag-epitope tagged SynCAM 1 under the control of a Tet-responsive element (TRE) (Mansuy and Bujard, 2000) (Figure 1A). This line was crossed to mice transgenically expressing the transcriptional transactivator tTA from the CaMKII promoter, which is active in excitatory forebrain neurons (Mayford et al., 1996). In the resulting TRE-SynCAM 1^{flag} x CaMKII-tTA mice, tTA mediated the expression of the transgenic SynCAM 1^{flag} protein throughout neurons in the forebrain, similar to its endogenous distribution (Figures S1A and S1B) (Thomas et al., 2008). Mice carrying only the CaMKII-tTA transgene did not exhibit altered SynCAM 1 protein levels (data not shown) and served as controls for transgenic SynCAM 1^{flag} overexpressors (OE) in this study.

The developmental profile of SynCAM 1^{flag} protein expression in OE mice followed the increase of endogenous SynCAM 1 in the postnatal forebrain, without altering the expression of SynCAM 2-4 (Figure 1B). No change in the expression profile of other synaptic proteins was detected (Figure 1B) and quantitative immunoblotting at P28 confirmed that the amounts of neuroligin 1, NCAM, and N-cadherin were unaltered in these mice (data not shown). Our transgenic design resulted in 8.4 ± 0.03-fold higher amounts of total SynCAM 1 in the hippocampus at P28, without affecting its expression in the cerebellum where the CaMKII promoter is inactive and tTA is not expressed (Figure 1C). This double-transgenic mouse model constitutes a Tet-Off system (Mansuy and Bujard, 2000) and administration of the tTA inhibitor doxycycline tightly repressed SynCAM 1^{flag} approximately to control levels (Figure 1C).

Synaptic Localization and Adhesive Interactions of Transgenic SynCAM 1

Subcellular fractionation confirmed the enrichment of overexpressed SynCAM 1 in synaptic plasma membranes purified from forebrain of adult OE mice, similar to endogenous SynCAM 1 in controls (Figure 1D). Consequently, total SynCAM 1 amounts were increased 8-fold in synaptic plasma membranes purified from the forebrain of adult OE mice (Figure S1C). Immunohistochemical analysis confirmed the correct subcellular sorting of SynCAM 1^{flag} to synaptic regions, while cell body layers lacked staining (Figure 1E). Analysis at higher magnification revealed that the majority of vGlut1/2-positive excitatory synapses expressed SynCAM 1^{flag} (Figure 1F), whereas it was not detected at inhibitory synapses marked by GAD65 (Figure 1G). This agreed with previous immunoelectron microscopic results that SynCAM proteins are endogenously present at excitatory synapses (Biederer et al., 2002). We additionally immunoprecipitated SynCAM 1 to test whether overexpression alters its extracellular interactions (Figure 1H). Control mice showed strong heterophilic interaction of SynCAM 1 with SynCAM 2 (lanes 1-4) as reported previously (Fogel et al., 2007). Overexpression of SynCAM 1 reduced the amount of bound SynCAM 2 (lanes 5–8), presumably because elevation of SynCAM 1 increased the formation of homophilic SynCAM 1 adhesion complexes and competed SynCAM 2 out of the heterophilic interaction. Heterophilic SynCAM 1/2 complexes were however still readily detected in the overexpressors, consistent with the coimmunoprecipitation of endogenous

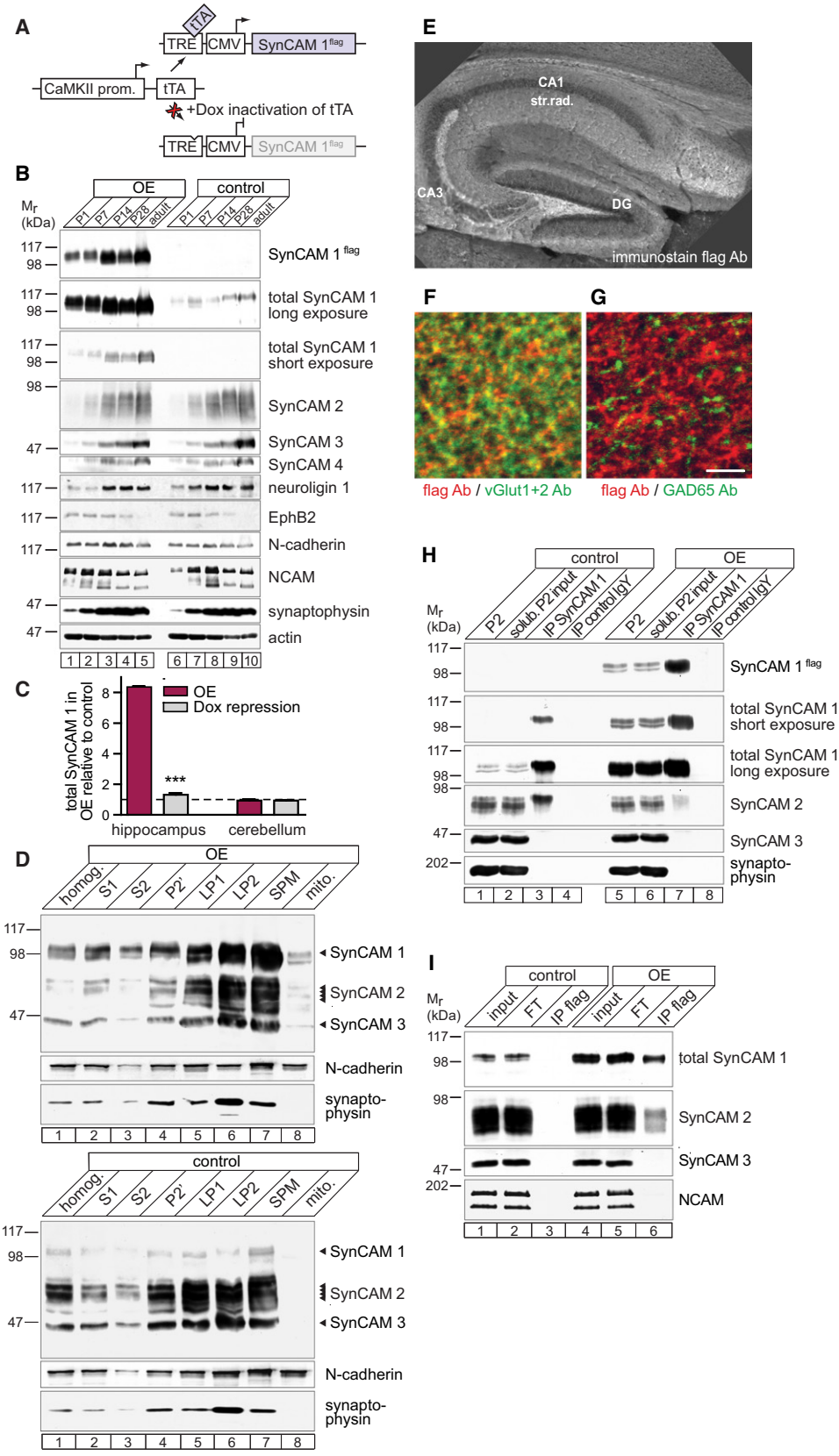
A
tTA
TRE
CMV
SynCAM 1 flag
CaMKII prom.
tTA
+Dox inactivation of tTA
TRE
CMV
SynCAM 1 flag
B
OE
control
Mr (kDa)
P1
P7
P14
P28
adult
SynCAM 1 flag
total SynCAM 1 long exposure
total SynCAM 1 short exposure
SynCAM 2
SynCAM 3
SynCAM 4
neuroligin 1
EphB2
N-cadherin
NCAM
synaptophysin
actin
C
total SynCAM 1 in OE relative to control
OE
Dox repression
***
hippocampus
cerebellum
D
OE
control
homog.
S1
S2
P2'
LP1
LP2
SPM
mito.
SynCAM 1
SynCAM 2
SynCAM 3
N-cadherin
synapto-physin
E
CA1
str.rad.
CA3
DG
immunostain flag Ab
F
G
flag Ab / vGlut1+2 Ab
flag Ab / GAD65 Ab
H
control
OE
P2
solub. P2 input
IP SynCAM 1
IP control IgY
SynCAM 1 flag
total SynCAM 1 short exposure
total SynCAM 1 long exposure
SynCAM 2
SynCAM 3
synapto-physin
I
control
OE
input
FT
IP flag
total SynCAM 1
SynCAM 2
SynCAM 3
NCAM

SynCAM 2 with overexpressed SynCAM 1^{flag} using anti-flag antibodies (Figure 1I). Together, this transgenic SynCAM 1 mouse model replicated the properties of endogenous SynCAM 1 and was suited to identify roles of SynCAM 1 in the postnatal brain.

SynCAM 1 Promotes the Number of Excitatory Synapses

Using electron microscopy, we determined the effects of altered SynCAM 1 expression on the density and ultrastructure of excitatory (Gray type I, asymmetric) and inhibitory (Gray type II, symmetric) synapses in the CA1 stratum radiatum of the hippocampus (Figures 2A and 2H). This area was selected as the morphological and physiological properties of its synapses are well characterized. Importantly, the density of excitatory synapses in SynCAM 1 overexpressing mice was increased by 26% ± 3%, while the number of the less abundant inhibitory synapses was not affected (Figure 2B). In addition, we used electron microscopy to count inhibitory synapses at perisomal regions of CA1 pyramidal neurons, where inhibitory synapses are prominent (Megias et al., 2001). As in CA1 stratum radiatum, no difference in perisomal inhibitory synapse density was observed between SynCAM 1 OE and control mice (Figures S2A and S2B). These results demonstrated that SynCAM 1 specifically increases excitatory synapse number. They also show that the elevation of SynCAM 1 in the complex environment of the brain is not compensated by mechanisms negatively regulating excitatory synapse number. Further, these findings agree with the synaptogenic activities of SynCAM 1 previously demonstrated in cultured hippocampal neurons (Biederer et al., 2002; Fogel et al., 2007; Sara et al., 2005). The absence of an effect on inhibitory synapse number in vivo was consistent with our transgenic design that overexpressed SynCAM 1 in excitatory forebrain neurons, similar to its endogenous expression pattern (Thomas et al., 2008). The average number of synaptic vesicles per excitatory terminal was not altered by SynCAM 1 overexpression (Figure 2C), and the thickness and length of the postsynaptic density (PSD) were also unchanged (Figures 2D and 2E). These results demonstrated that SynCAM 1 overexpression increases excitatory synapse number in vivo without altering their ultrastructure.

We considered that our electron microscopic study was likely biased toward excitatory synapses on mushroom-type spines as these are most prominent and readily identifiable. For a comprehensive analysis of all spine types, we employed Golgi staining (Figure 2F) and classified spines of pyramidal neurons in CA1 stratum radiatum using described criteria (Knott et al., 2006). This demonstrated an increase in total spine density by 37% ± 10% in SynCAM 1 overexpressors. Morphometric scoring determined a 34% ± 10% increase in the density of mushroom-type spines per dendrite length, and a 4-fold increase in the number of the far less prominent thin spines (Figure 2G). The density of stubby spines and the small fraction of unclassifiable spine structures was unchanged (data not shown). These results agree with our electron microscopic analysis and additionally revealed an increased number of thin spines, which can correspond to sites of new synapses (Knott et al., 2006; Ziv and Smith, 1996).

Endogenous SynCAM 1 Regulates Excitatory Synapse Number and Structure

The effects of SynCAM 1 overexpression motivated us to analyze synapses in the brain of KO mice lacking SynCAM 1 to determine whether the organization of synapses is its endogenous function. The only previously known phenotype of SynCAM 1 KO neurons is their more exuberant growth cone morphology in early development (Stagi et al., 2010), while synaptic changes remained to be addressed. The one apparent phenotype of these KO mice is male infertility due to impaired spermatid adhesion (Fujita et al., 2006). Our electron microscopic analysis of the hippocampal CA1 stratum radiatum at P28 showed that the number of excitatory synapses in SynCAM 1 KO mice was significantly reduced by 10% ± 3% (Figure 2I), demonstrating that it is a biological function of SynCAM 1 to contribute to synapse organization. As in SynCAM 1 overexpressors, the number of inhibitory synapses was neither affected in the CA1 stratum radiatum of KO mice (Figure 2I) nor in the stratum pyramidale (Figures S2C and S2D). The PSD length was reduced in SynCAM 1 KO mice by 19% ± 2%, concomitant with a reduction in active zone length by 15% ± 3%, while other parameters of synapse ultrastructure were unchanged (Figures 2J–2M). Electron microscopic analysis demonstrated that the presynaptic terminal area was unchanged in the KO (data not shown), indicating that these

Figure 1. Development of a Transgenic SynCAM 1 Mouse Model

(A) SynCAM 1 Tet-Off transgenic design. The CaMKII promoter restricts expression of the transcriptional transactivator tTA to excitatory forebrain neurons. tTA binds a Tet-responsive element (TRE) to drive flag-tagged SynCAM 1. Doxycycline (Dox) inhibits tTA.

(B) Transgenic SynCAM 1^{flag} expression in forebrain (lanes 1–5) follows the endogenous profile (lanes 6–10) as shown by immunoblotting. Other synaptic proteins are unchanged. P, postnatal day.

(C) Transgenic expression elevates SynCAM 1 in hippocampus as analyzed by quantitative immunoblotting at P28. Overexpression (OE) occurred until P28 or was repressed with Dox from P14 until 28. Signals were normalized to littermate controls carrying only the tTA transgene. Statistical analysis was performed using Student's t test with errors corresponding to the standard error of the mean (SEM). ***$p < 0.001$.

(D) SynCAM 1^{flag} (OE, top) fractionates with synaptic plasma membranes (SPM) similar to endogenous SynCAM 1 (tTA control, bottom). SynCAM 1-3 were detected at their distinct molecular weights with a pleio-antibody. N-cadherin marks SPM and synaptophysin marks synaptic vesicles (LP2). SynCAM 1 and 2 are present in LP2 due to nonvesicular fractions (Fogel et al., 2007). S, supernatant; P, pellet; LP, lysis pellet; mito, mitochondria.

(E–G) SynCAM 1^{flag} is sorted to excitatory synapses as analyzed at P21. (E) Anti-flag immunostaining of CA1 stratum radiatum and CA3 mossy fiber terminals of hippocampus. DG, dentate gyrus. (F and G) SynCAM 1^{flag} localizes to excitatory but not inhibitory synapses. Both panels show the same triple-labeled hippocampal section at P21. Red marks flag staining in both panels and green represents either vGlut-positive excitatory synapses (F) or GAD65-positive inhibitory synapses (G). Scale bar represents 5 μm.

(H) Coimmunoprecipitation (IP) of SynCAM 2 with SynCAM 1 from synaptosomes at P55 is reduced in SynCAM 1 OE compared to controls. SynCAM 3 and synaptophysin were negative controls. Input lanes contain 5% of the extract used for the IP. Same results were obtained at 12 months. P2, synaptosomes.

(I) SynCAM 2 is coimmunoprecipitated with overexpressed SynCAM 1^{flag} using flag antibodies. Input from tTA animals served as negative control for the IP.

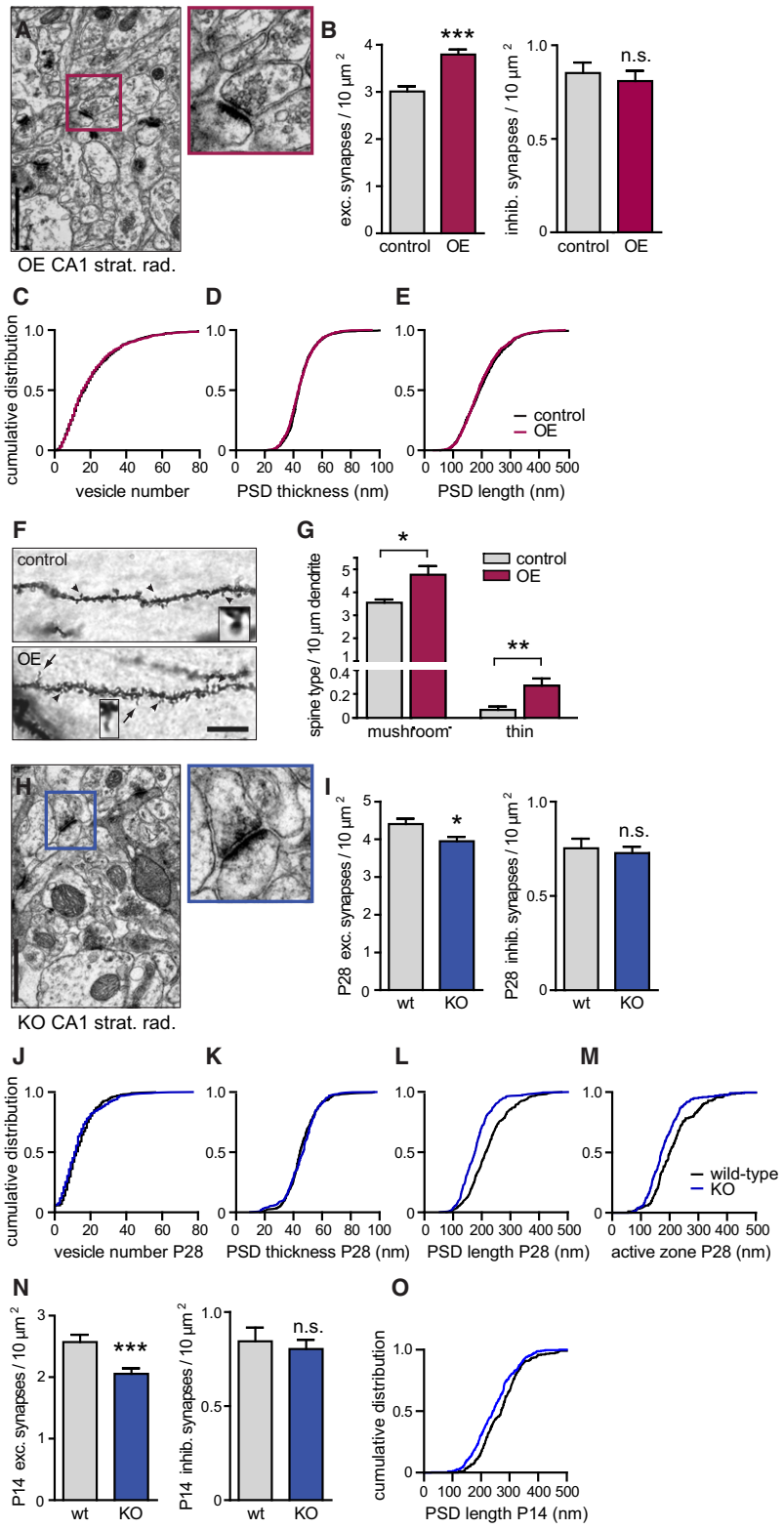

Figure 2. SynCAM 1 Regulates Excitatory Synapse Number

(A–E) Electron microscopy of synapses in CA1 stratum radiatum of SynCAM 1 overexpressors (OE) at 12–15 months. (A) Left, micrograph of overexpressors (magnification = 26,500×). Right, excitatory synapse boxed on the left. Scale bar in (A) and (H), 1 µm. (B) SynCAM 1 overexpression increases excitatory synapse density. (tTA controls, n = 180 images, 848 synapses, 3 male littermates; OE, n = 180 images, 1087 synapses, 3 males) Inhibitory synapse density is unaffected by overexpression. (tTA controls, n = 122 images, 160 synapses, 3 males; OE, n = 95 images, 119 synapses, 3 males). (C–E) Elevated SynCAM 1 at excitatory synapses alters neither (C) average synaptic vesicle number per terminal (tTA controls 21 ± 0.6, n = 793 synapses; OE 21 ± 0.6, n = 1018), (D) PSD thickness (tTA controls 45 ± 0.4 nm, n = 846; OE 45 ± 0.3 nm, n = 1087), nor (E) PSD length (tTA controls 204 ± 3 nm, n = 846; OE 200 ± 2 nm, n = 1087). Distributions were identical by the Kolmogorov-Smirnov (KS) test (p = 1 in C–E).

(F and G) Golgi staining in CA1 stratum radiatum at 5 months. (F) Apical secondary and tertiary dendrites of tTA controls (top) and SynCAM 1 OE (bottom). Arrowheads point to mushroom-type spines and arrows to thin spines, with examples enlarged. Scale bar represents 10 µm. (G) Higher mushroom-type and thin spine density in SynCAM 1 OE. (tTA controls, n = 422 spines, 3 male littermates; OE, n = 757, 3 males).

(H–M) Electron microscopic analysis of synapses in CA1 stratum radiatum of SynCAM 1 KO mice at P28. (H) Micrograph of KO mice (magnification = 26,500×) with one excitatory synapse enlarged. (I) SynCAM 1 KO mice have fewer excitatory synapses. (wild-type, n = 120 images, 825 synapses, 2 male littermates; KO, n = 180 images, 1110 synapses, 3 males) Lack of SynCAM 1 affects neither (I) inhibitory synapse density (wt, n = 24 synapses; KO, n = 40), (J) synaptic vesicle number per terminal (wt 14 ± 0.5, n = 391 synapses; KO 13 ± 0.6, n = 302), nor (K) PSD thickness (wt 46 ± 0.6 nm, n = 391; KO 46 ± 0.7 nm, n = 302; KS test p = 1 in L, M). (L) SynCAM 1 KO shortens PSDs (wt 224 ± 4 nm, n = 391 synapses; KO 182 ± 4 nm, n = 302) and (M) active zones (wt 216 ± 6 nm, n = 180; KO 184 ± 4 nm, n = 236; KS test p < 0.001 in L, M).

(N and O) Electron microscopy of synapses in CA1 stratum radiatum of SynCAM 1 KO mice at P14. (N) Lack of SynCAM 1 reduces excitatory synapse number already at P14. (wild-type, n = 53 images, 211 synapses, 2 male littermates; KO, n = 92 images, 293 synapses, 2 males) but does not affect inhibitory synapse density (wt, n = 68 synapses; KO, n = 117) (O) SynCAM 1 KO shortens PSDs already at P14 (wt 269 ± 5 nm, n = 208 synapses; KO 243 ± 4 nm, n = 306; KS test p < 0.01).

Statistical analyses in (B), (G), (I), and (N) were performed using Student's t test with errors corresponding to SEM. *p < 0.05; **p < 0.01; ***p < 0.001.

ultrastructural effects of SynCAM 1 loss result from impaired interactions across the synaptic cleft and are not due to a nonspecific reduction of synapse size.

To address the developmental roles of SynCAM 1 at synapses, we analyzed KO mice at P14. Similar to the results at P28, the lack of SynCAM 1 reduced the number of excitatory

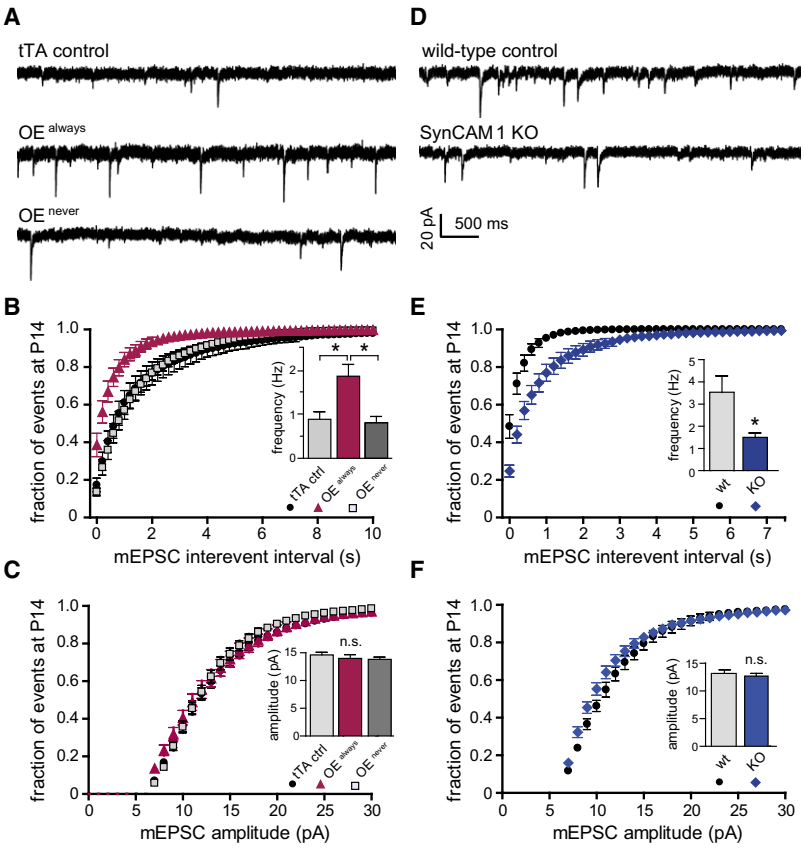

Figure 3. SynCAM 1 Promotes Functional Excitatory Synapses

Whole-cell mEPSC recordings from hippocampal CA1 pyramidal neurons at P15-19.

(A–C) Analysis of mice continuously overexpressing SynCAM 1 (OE^{always}), mice in which SynCAM 1 overexpression was continuously repressed by doxycycline (OE^{never}), and tTA littermate controls. (A) Representative traces. (B) Cumulative distributions of mEPSC interevent intervals. mEPSC frequency is strongly increased in OE^{always} mice compared to tTA controls and OE^{never} mice. The inset shows average frequencies. (KS test $p < 0.001$ for OE^{always} versus tTA and OE^{always} versus OE^{never}, $p > 0.1$ for OE^{never} versus tTA; tTA n = 14; OE^{always} n = 11; OE^{never} n = 12). (C) mEPSC amplitudes are unaltered by SynCAM 1 overexpression. (tTA controls n = 11; OE^{always} n = 14; OE^{never} n = 12).

(D–F) mEPSC recordings from wild-type control and SynCAM 1 knockout littermates at P14-15. (D) Representative traces. Scale bar in (D) applies to (A) and (D). (E) Loss of SynCAM 1 decreases excitatory synapse number. Cumulative distributions of mEPSC interevent intervals show a strong reduction of mEPSC frequency in SynCAM 1 KO mice compared to wild-type littermates (KS test $p < 0.001$). The inset depicts average mEPSC frequencies. (wild-type n = 16; KO n = 8) Different mEPSC frequencies in tTA controls in (B) and controls in (E) are likely due to genetic background differences of these strains (see Supplemental Experimental Procedures). (F) mEPSC amplitudes of SynCAM 1 KO (n = 16) mice are not significantly changed compared to wild-type littermates (n = 8). Statistical analyses in (B), (C), (E), and (F) were performed using Student's t test with errors corresponding to SEM. * $p < 0.05$; n.s., not significant.

synapses by 20% ± 6%, while inhibitory synapse density was unchanged (Figure 2N). PSD length was also shortened by 9% ± 2% (Figure 2O). SynCAM 1 therefore modulates excitatory synapse number at different stages of postnatal development. Moreover, our findings show that endogenous SynCAM 1 not only elevates synapse number but also plays a role in the structural organization of excitatory synapses.

We noted a higher density of excitatory synapses in wild-type controls of the KO mice compared to the transgenic controls containing the tTA transgene alone (Figures 2B and 2I). This likely reflects the different genetic backgrounds of the KO and transgenic mouse strains used in this study. A rescue of the SynCAM 1 KO by transgenic overexpression was not performed because the male infertility of the KO left only breeding strategies with a very low likelihood of obtaining litters that included offspring carrying the SynCAM 1 gene deletion and both transgenes encoding SynCAM 1^{flag} and tTA, and the required littermate controls. Together, the reciprocal effects of overexpression and loss on synapse density in these mouse models demonstrate that SynCAM 1 promotes excitatory synapse numbers in vivo.

SynCAM 1-Induced Synapses Are Functional

We next addressed whether the synapses gained by SynCAM 1 overexpression were functional. We used miniature excitatory postsynaptic current (mEPSC) frequency as a measure of synapse number, as an increase in the number of functional synapses would increase the frequency of mEPSCs. Recordings were obtained from acute hippocampal slices at P14. Similar to the morphological data, we observed strain-dependent mEPSC differences between overexpressor and KO controls. We therefore only compared relative differences of overexpressors and KOs to their respective littermate controls. Consistent with the increase in morphologically defined synapses, transgenic animals continuously overexpressing SynCAM 1 (OE^{always}) exhibited a strong 2.1-fold increase in mEPSC frequency compared to control littermates carrying only the tTA transgene (Figures 3A and 3B). mEPSC amplitude was not affected (Figure 3C). The transgenic design allowed us to continuously repress overexpression by administering doxycycline (see Figures 1C and 5B). These doxycycline-treated mice served as additional controls (OE^{never}) and their mEPSC frequencies and amplitudes were indistinguishable from those of tTA control littermates (Figures 3A–3C).

Converse to the overexpression of SynCAM 1, its loss caused a strong reduction in mEPSC frequency by more than half compared to control wild-type littermates (Figures 3D and 3E). The unaltered mEPSC amplitude in the KO mice (Figure 3F) indicated that the density of AMPA receptors is not changed in their shortened PSD, as mEPSC amplitude reflects AMPA receptor density rather than total receptor number (Raghavachari and Lisman, 2004). A similar phenotype of reduced PSD length and

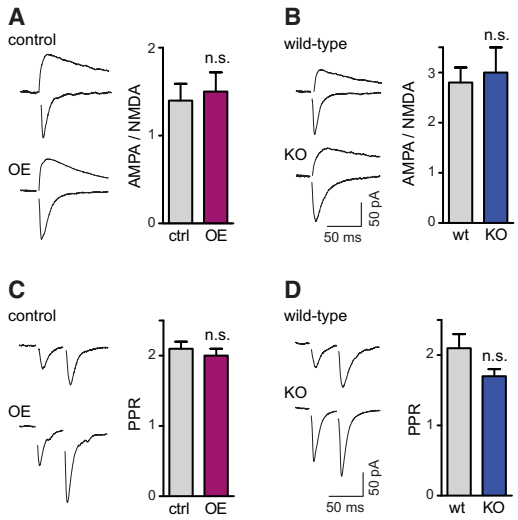

Figure 4. SynCAM 1 Does Not Alter Basal Synaptic Transmission

(A and B) Left, representative traces of AMPA and NMDA currents from CA1 neurons at P15–19. Right, synaptic strength is unaffected by SynCAM 1 because AMPA/NMDA ratios are neither altered by SynCAM 1 overexpression (A; tTA controls n = 7; OE n = 8; $p > 0.5$) nor its loss (B; wild-type n = 12; KO n = 13; $p > 0.6$). Scale bar in (B) applies to (A) and (B).

(C and D) Paired-pulse ratio (PPR), a measure for short-term plasticity of presynaptic release, is neither altered by SynCAM 1 overexpression (C; tTA controls n = 17; OE n = 15; $p > 0.5$) nor its absence (D; wild-type n = 17; KO n = 11; $p > 0.1$). Scale bar in (D) applies to (C) and (D).

Statistical analyses in (A)–(D) were performed using Student's t test with errors corresponding to SEM. n.s., not significant.

unaltered mEPSC amplitude has also been observed in Shank1 KO mice (Hung et al., 2008). We noticed that the effect of SynCAM 1 on mEPSC frequency is more pronounced than on synapse number. One reason may be that synapses rendered nonfunctional by the absence of SynCAM 1 could appear normal on the morphological level such as reported for Munc-18-1 KO and neuroligin 1-3 KO mice (Varoqueaux et al., 2006; Verhage et al., 2000). Taken together, these electrophysiological data revealed that SynCAM 1 levels regulate the number of functional excitatory synapses.

Other Steady-State Synaptic Properties Are Unaffected by SynCAM 1

Does SynCAM 1 affect other functional synaptic properties? To assess synaptic strength, we analyzed the α-amino-3-hydroxy-5-methyl-4-isoxazole propionic acid (AMPA) receptor and N-methyl-D-aspartate (NMDA) receptor components of evoked excitatory postsynaptic currents (EPSC). Compared to their respective littermate controls, the AMPA/NMDA ratio was neither altered in SynCAM 1 overexpressors (Figure 4A) nor in KO animals (Figure 4B). Analyzing presynaptic properties, we found that the paired-pulse ratio (PPR), a measure of changes in the probability of transmitter release, was unchanged after SynCAM 1 overexpression or loss (Figures 4C and 4D). The increase in mEPSC frequency in SynCAM 1 overexpressors therefore likely reflects higher excitatory synapse numbers rather than an elevated release probability. Together with the ultrastructural analyses, these results showed that most structural and basic functional properties of synapses are intact under conditions of SynCAM 1 overexpression or loss, with the exception of the shortened PSD in the KO. This lack of changes in parameters associated with synapse maturation indicated a select effect of SynCAM 1 on synapse number.

SynCAM 1 Sustains the Increase in Excitatory Synapse Number

We wanted to determine at which point in the lifetime of synapses SynCAM 1 acts and considered two hypotheses: first, SynCAM 1 functions only at early stages of synapse development to increase synapse number and is then dispensable. In this first case, the SynCAM 1-mediated increase in synapse number would persist beyond a shutdown of its overexpression. We also considered as a second hypothesis that SynCAM 1 could be continuously required to sustain excitatory synapses number, possibly by initially promoting excitatory synapse formation and then maintaining them. In that second case, the gain in synapse number would be lost after ending SynCAM 1 overexpression.

To distinguish between these hypotheses, we utilized the temporal expression control afforded by our transgenic mouse model. SynCAM 1 overexpression effects on mEPSC frequency were compared at P14 and P28, i.e., during and after the peak of synaptogenesis. Three different experimental conditions were analyzed. Animals overexpressed SynCAM 1 either constitutively (OE^{always}), or only within the first 2 weeks of postnatal development until P14 (OE^{early}), or selectively from P14–P28 (OE^{late}) (Figure 5A). Immunoblotting of hippocampal lysates obtained after these treatments confirmed the intended repression and induced expression of SynCAM 1^{flag} (Figure 5B). Three controls were analyzed in parallel. In the first cohort of controls, SynCAM 1 overexpression was continuously repressed by administering doxycycline (OE^{never}). A second and third cohort comprised mice carrying only tTA and lacking the SynCAM 1 transgene. This second group of controls remained untreated, while the third control group was treated with doxycycline to exclude nonspecific effects of this drug on synapse number. mEPSC frequencies and amplitudes were indistinguishable under all control conditions (Figure S3).

As observed at P14 (see Figure 3B), the continuous overexpression of SynCAM 1 until P28 caused a strong increase in mEPSC frequency (Figures 5C and 5D). Interestingly, when the overexpression of SynCAM 1 was repressed until P14 but switched on at P14 (OE^{late}), we observed at P28 an increased mEPSC frequency that was statistically indistinguishable from continuous overexpression (Figure 5D). This indicates that SynCAM 1 can increase synapse number also at later stages of postnatal development. Importantly, when SynCAM 1 was overexpressed until P14, but was then shut down (OE^{early}), mEPSC recordings at P28 revealed that the increase in synapse number that had been observed at P14 was lost by P28 (Figures 5C and 5D). These results supported our second hypothesis that SynCAM 1 is required to sustain the increase in excitatory synapses it mediates.

Are these dynamic, SynCAM 1-dependent changes in functional excitatory synapse number also reflected on the

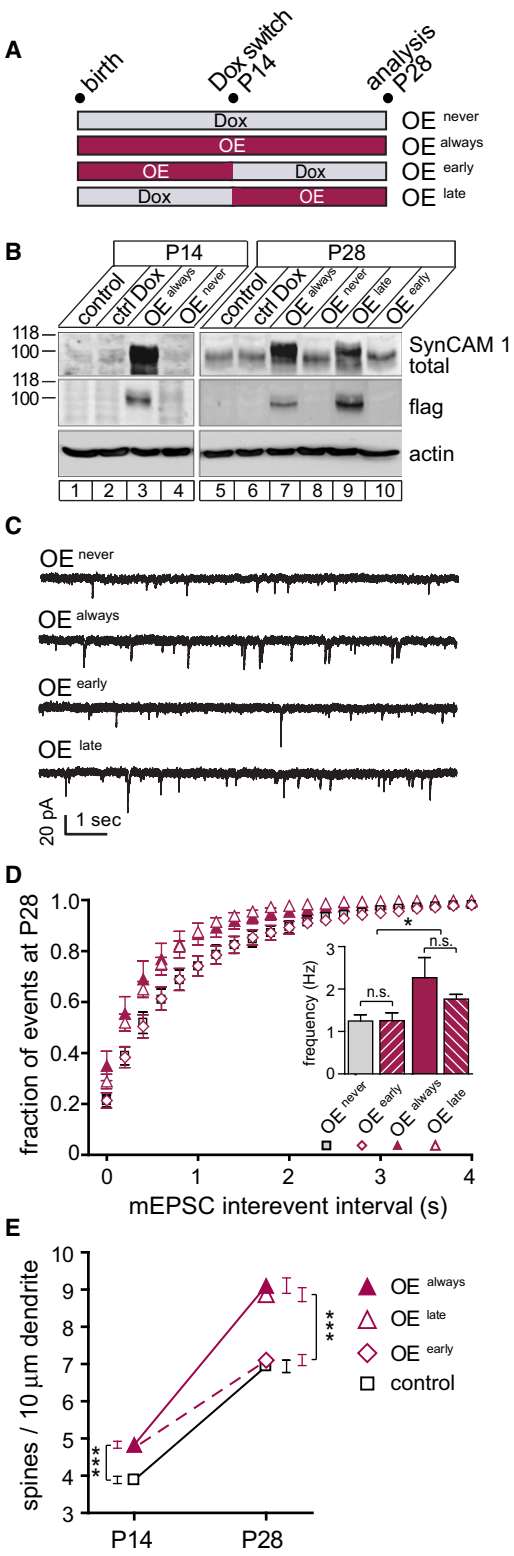

Figure 5. Continuous SynCAM 1 Presence Is Required to Maintain Increased Synapse Number

(A) Experimental design. SynCAM 1 overexpression was either continuously repressed by Dox treatment (OE^{never}), or occurred continuously until P28 (OE^{always}). Cohorts were treated with Dox from P14 to repress overexpression (OE^{early}), or were removed from Dox at P14 (OE^{late}) to turn overexpression on.

(B) Hippocampal homogenates from animals treated as in (A) were probed by immunoblotting. At P14, SynCAM 1^{flag} was only detected in OE^{always} mice. At P28, SynCAM 1^{flag} is repressed to undetectable levels in both OE^{early} and OE^{never} conditions. SynCAM 1^{flag} amounts reach maximum by P28 even when overexpression was only initiated from P14 on (OE^{late}). Actin served as a loading control.

(C) Representative mEPSC traces from P28 hippocampal CA1 neurons after treatments as in (A).

(D) The SynCAM 1-induced increase in synapses requires its presence to be maintained. OE^{always} mice exhibit increased mEPSC frequency at P28 compared to OE^{never} controls. Overexpression of SynCAM 1 increases mEPSC frequencies at P14 (see Figure 3B), but subsequent repression returns frequencies to control levels by P28 (OE^{early}). When overexpression is turned on at P14 (OE^{late}), mEPSC frequencies are indistinguishable from OE^{always} mice. mEPSC frequencies in OE^{never} mice are identical to littermate controls carrying only the tTA transgene (see Figures S3A and S3B). For statistical comparisons, see Figures S3C and S3F.

(E) Maintaining the SynCAM 1-induced spine increase requires its presence. Overexpression of SynCAM 1 until P14 increases spines densities over tTA littermate controls. At P28, OE^{always} mice similarly show increased spine densities over tTA controls. Turning SynCAM 1 overexpression on at P14 (OE^{late}) results at P28 in spine densities that are identical to OE^{always} mice. Repression of SynCAM 1 overexpression from P14 (OE^{early}) reduces spine densities to control levels by P28 (dashed line). Spine densities in OE^{never} mice are identical to tTA littermate controls (see Figure S4A). For statistical comparisons, see Figure S4B.

Statistical analyses in (D) and (E) were performed using Student's t test with errors corresponding to SEM. *p < 0.05; ***p < 0.001; n.s., not significant.

morphological level? To address this, we analyzed Golgi-stained spines as a measure of excitatory synapses. Employing the same temporally controlled expression as for the mEPSC analysis, we determined that spine densities were indistinguishable under all control conditions at P28 (Figure S4). The overexpression of SynCAM 1 until P14 resulted in a significant increase in total spine density by 31% ± 3% compared to tTA littermate controls (Figure 5E), similar to the spine increase in adult OE mice (see Figure 2G). These SynCAM 1 overexpressing P14 mice also exhibited a 5-fold increase in the small fraction of thin spines over controls (data not shown). Similarly, overexpression of SynCAM 1 until P28 increased total spine density by 24% ± 2%. The same increase was determined in OE^{late} mice (Figure 5E), demonstrating that SynCAM 1 can increase excitatory synapse number even after the peak of synaptogenesis has been reached around P14. Importantly, the spine gain caused by elevating SynCAM 1 until P14 was lost at P28 on shutdown of overexpression in OE^{early} mice. Together, both the electrophysiological measurement of functional excitatory synapses and the Golgi staining of spines demonstrated that the continued elevation of SynCAM 1 is necessary to maintain the increase in excitatory synapses it drives in the first place.

Long-Term Depression Is Regulated by SynCAM 1 Expression Levels

Trans-synaptic interactions may not only alter synapse formation and development but also synaptic plasticity. Long-term depression (LTD), a plasticity mechanism that decreases synaptic strength after low-frequency stimulation, correlates with spine shrinkage (Zhou et al., 2004). Considering the effects

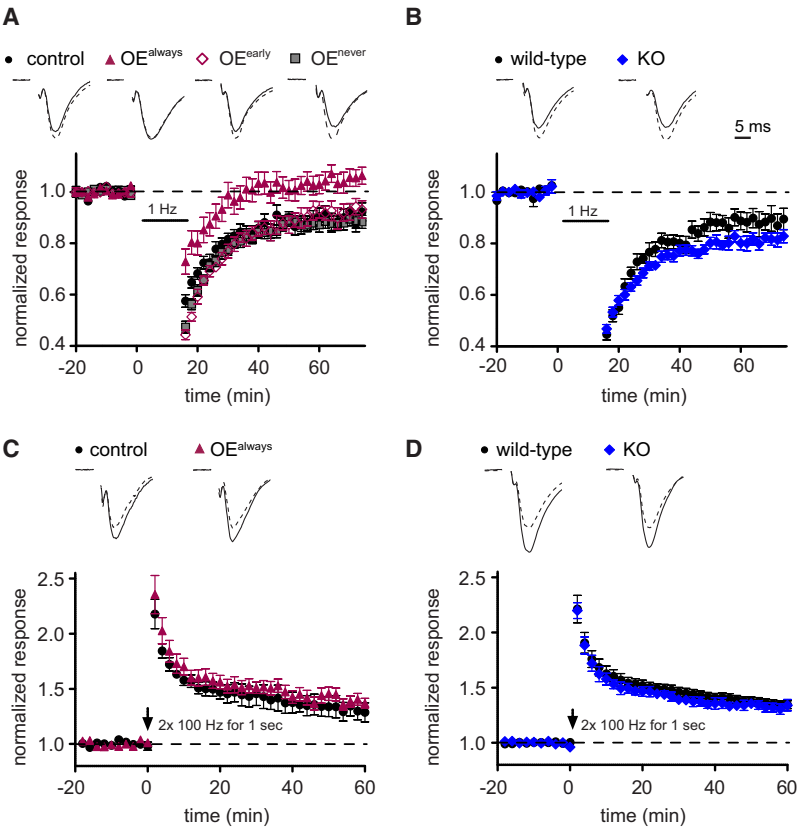

Figure 6. SynCAM 1 Restricts Long-Term Depression

(A and B) Extracellular field potential recordings (fEPSPs) were obtained before and after induction of LTD in SynCAM 1 overexpressors (A) and KO mice (B). Top, representative fEPSP traces show normalized average fEPSPs before (dashed line) and after LTD induction (solid line). (A) LTD is absent in SynCAM 1 overexpressors, while tTA control animals exhibit normal LTD. Shutting down SynCAM 1 overexpression continuously (OE^{never}) or after P8 (OE^{early}) rescues the loss of LTD observed in SynCAM 1 overexpressors (OE^{always}). Note that LTD recordings from rescue and control animals are indistinguishable ($p > 0.1$) and are superimposed in the graph. (tTA controls 0.90 ± 0.01, $n = 15$; OE^{always} 0.99 ± 0.01, $n = 20$; $p < 0.001$, OE^{early} 0.92 ± 0.02, $n = 7$; OE^{never} 0.88 ± 0.01, $n = 19$) (B) Loss of SynCAM 1 increases LTD. (wild-type littermate controls 0.88 ± 0.01, $n = 10$; KO 0.82 ± 0.01, $n = 17$; $p < 0.001$).

(C and D) Overexpression (C) or loss (D) of SynCAM 1 do not affect LTP. Top, representative fEPSP traces show normalized average fEPSPs before (dashed line) and after LTP induction (solid line). (C, tTA littermate controls 1.29 ± 0.09, $n = 6$; OE 1.37 ± 0.05, $n = 10$; $p > 0.05$; D, wild-type littermate controls 1.34 ± 0.06, $n = 4$; KO 1.35 ± 0.04, $n = 10$; $p > 0.05$) Scale bar in (B) applies to all panels.

of SynCAM 1 on maintaining spine numbers, we tested whether SynCAM 1 expression modulates the activity-dependent weakening of synapses. Intriguingly, extracellular field potential recordings from the CA1 area of the hippocampus identified that mice continuously overexpressing SynCAM 1 (OE^{always}) failed to exhibit LTD (Figure 6A). We again used the temporal expression control of our transgenic mouse model and tested whether this impairment of LTD requires the continuous overexpression of SynCAM 1. Our results show that LTD was restored at P14 when SynCAM 1 overexpression was turned off from P8 on (OE^{early}) (Figure 6A). As expected, continuously repressed animals (OE^{never}) did not exhibit a change in LTD.

As we detected opposite effects of SynCAM 1 overexpression and loss on synapse numbers, we hypothesized that SynCAM 1 KO mice may show increased LTD reciprocal to the lack of LTD in the overexpressors. Indeed, LTD was expressed more strongly in SynCAM 1 KO mice (Figure 6B). These findings indicate a direct modulatory effect of SynCAM 1 overexpression and loss on this plasticity mechanism.

To test whether SynCAM 1 also alters the ability to strengthen synaptic transmission in an activity-dependent manner, we measured long-term potentiation (LTP) using a robust tetanic stimulation protocol. We observed no effects of SynCAM 1 overexpression or SynCAM 1 loss on LTP (Figures 6C and 6D). Together, these experiments demonstrated that the weakening of synaptic connections by LTD is selectively and strongly affected by SynCAM 1.

SynCAM 1 Impacts Spatial Learning

As cognitive tasks involve synaptic plasticity (Nelson and Turrigiano, 2008; Neves et al., 2008), the synapse-organizing roles of SynCAM 1 may alter experience-dependent behaviors. We addressed this question first in the SynCAM 1 overexpressing mice that lacked LTD. Control experiments confirmed that their motor functions as well as vision were unaffected, permitting these behavioral studies (Figure 7A; Figures S5A–S5C). We tested these mice in the Morris water maze paradigm, a hippocampus-dependent task of spatial reference learning. The animals' motivation to reach a submerged, but visibly marked platform in a water tank was unaltered (Figures S6A and S6B). Notably, SynCAM 1 overexpressors failed to properly learn the target quadrant's location when the platform was hidden (Figure S6C), and correspondingly were unable to remember the correct maze quadrant when subjected to a probe trial (Figure 7B). This surprising impairment of spatial learning and memory was not due to a general hippocampal dysfunction, as these animals performed normally in a modified novel objection recognition task (Figure S6G). To extend this analysis beyond cognitive tasks, we also assessed anxiety-related behavior. Testing the SynCAM 1 overexpressing animals in the elevated plus maze identified no alteration in the number of entries into an exposed maze arm, indicative of unchanged anxiety levels (Figure S6H).

In contrast to SynCAM 1 overexpressors, LTD was enhanced in SynCAM 1 KO animals. This led us to hypothesize that learning might be altered and possibly improved in these mice. To facilitate the detection of putative improvements, behavioral studies were performed in aged mice as older rodents exhibit impaired spatial memory (Gage et al., 1989), which is apparent in the high error rate of aged wild-type mice (see Figure S6F). Motor

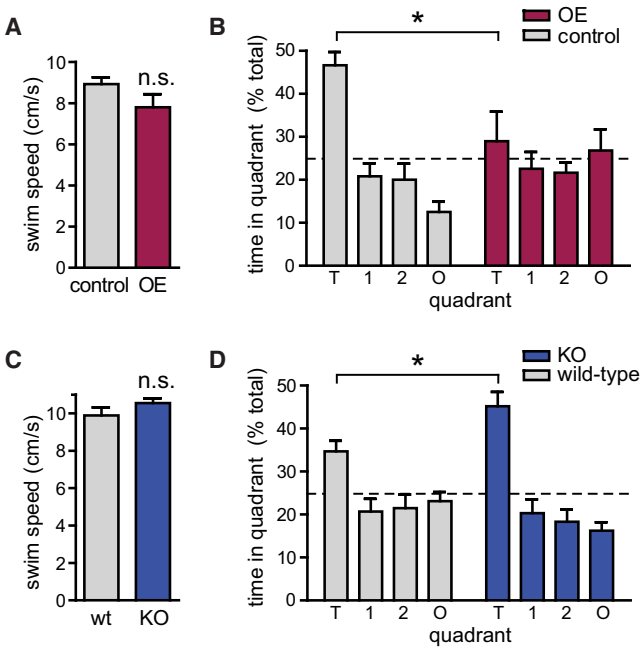

Figure 7. Spatial Learning Is Impaired by SynCAM 1 Overexpression and Enhanced by Its Loss

(A) Locomotor activity, measured by swim speed, is not altered in SynCAM 1 overexpressors. Results were obtained from 11 tTA littermate control and 12 SynCAM 1 OE male mice at 3–5 months.

(B) Spatial reference memory is impaired in SynCAM 1 overexpressors. After Morris water maze training, the time spent by mice in the target quadrant (T) was measured. Unlike controls, SynCAM 1 overexpressors exhibit no learned preference. Results were obtained from 11 tTA littermate control and 12 SynCAM 1 OE male mice at 4–5 months. O, opposite quadrant; 1, 2, adjacent quadrants. Dotted line indicates chance level.

(C) Swim speed is not altered in the SynCAM 1 KO. Results were obtained from eight wild-type littermate control and nine SynCAM 1 KO male mice at 6–12 months.

(D) SynCAM 1 KO mice exhibit better spatial reference memory. After training, KO mice spend more time in the Morris water maze target quadrant than controls. Results were obtained from seven wild-type littermate control and nine SynCAM 1 KO male mice at 6–12 months. Differences in time spent in quadrant T by tTA controls in (B) and controls in (D) are likely due to their different age and genetic background.

Statistical analyses in (A)–(D) were performed using Student's t test with errors corresponding to SEM. *$p < 0.05$; n.s., not significant.

functions were normal in aged KO mice (Figure 7C; Figure S5D), and no changes in anxiety-related behavior were identified (Figure S6I). Furthermore, the animals' motivation to reach the visibly marked platform in a water tank was unaffected (Figures S6D and S6E). We were intrigued to observe that SynCAM 1 KO mice learned the location of the correct quadrant in the Morris water maze significantly faster than wild-type littermate controls (Figure S6F). Even more surprisingly, these trained SynCAM 1 KO mice exhibited significantly enhanced spatial memory (Figure 7D).

DISCUSSION

Our results reveal that the synaptic adhesion molecule SynCAM 1 contributes to the regulation of excitatory synapses in the brain in two distinct ways, through altering their number as well as their plasticity. Consistent with its expression into adulthood, SynCAM 1 regulates excitatory synapse number both in the developing and adult brain as measured by electron microscopy, Golgi staining, and electrophysiology. SynCAM 1 not only increases excitatory synapse density but its expression is additionally required to maintain this increase as shown using temporally controlled overexpression. Moreover, the analysis of SynCAM 1 KO mice reveals that its loss results in fewer excitatory synapses with a shortened PSD. Our results in OE and KO mouse models demonstrate that the organization of excitatory synapses is a key developmental role of SynCAM 1 and indicate that its expression directly regulates synapse number. Notably, SynCAM 1 also changes synaptic plasticity through restricting LTD. These effects correlate with behavioral changes, and SynCAM 1 KO animals perform better than wild-types in spatial learning. In contrast, the overexpressing mice that lack LTD are unable to acquire this form of reference memory. Our findings demonstrate that SynCAM 1 organizes excitatory synapses by contributing to the regulation of both their number and synaptic plasticity. This distinguishes it from proteins such as neuroligins that serve in synapse maturation in vivo (Varoqueaux et al., 2006).

With respect to synapse development, this work provides new insights into *trans*-synaptic interactions by demonstrating that SynCAM 1 organizes synapses in the brain. Based on our results, and the contribution of adhesive SynCAM 1 assembly to axo-dendritic contact formation (Stagi et al., 2010), we propose that SynCAM 1 participates both in early steps of synaptogenesis and subsequently in maintaining this increase in excitatory synapse number. Mechanistically, SynCAM 1 adhesion may drive excitatory synapses by promoting the prolonged structural interactions between axon and dendrite that precede excitatory, but not inhibitory, synapse formation (Wierenga et al., 2008). Here, an increase of homophilic SynCAM 1/1 complexes in transgenic overexpressors that is paralleled by the reduction in SynCAM 1/2 complexes may stabilize nascent synapses to increase synapse number. This molecular change in SynCAM adhesion complexes may therefore specifically impact synaptic differentiation.

Interestingly, the absence of SynCAM 1 already resulted in a significant reduction of synapse number, despite the continued expression of the three other members of this protein family. This demonstrated that its loss is not fully compensated by these or other synapse-organizing proteins. This was unexpected because SynCAM 1 is expressed at lower protein amounts than SynCAM 2, and may reflect a select role of SynCAM 1 in the adhesive stabilization of excitatory synapses. The acute loss of SynCAM 1 may impact the number of synapses even more strongly, but this could not be addressed as our studies were performed in a constitutive SynCAM 1 KO. Similarly, our analysis of the inducible transgenics showed that other synapse-organizing proteins did not compensate for the absence of overexpressed SynCAM 1 once it was shut down in OE^{early} mice. This resulted in the loss of the SynCAM 1-induced increase in synapse number we measured by electrophysiological recordings and Golgi staining of spines. These

findings point to specific roles of SynCAM 1 compared to other synaptic adhesion molecules, and underline that SynCAM 1 acts in a partially nonredundant manner, unlike reported for neuroligins (Chih et al., 2005; Varoqueaux et al., 2006). These consequences of SynCAM 1 elevation and loss are reminiscent of the dose-dependent effects of the homophilic Ig adhesion molecule fasciclin II on synapse formation in *Drosophila* (Davis et al., 1997).

SynCAM 1 likely organizes excitatory synapses throughout development and into adulthood. This is indicated by the reduction of synapse number both during the peak of synapse formation at P14 and once most synapses have formed at P28 as observed by electron microscopy. Our physiological recordings in the developing brain of KO mice support this conclusion. Roles in the mature brain are consistent with the increase in synapse number even if SynCAM 1 is overexpressed only in later postnatal development, i.e., subsequent to the peak of synaptogenesis. Interestingly, functions of SynCAM 1 in the adult brain have been independently indicated by the upregulation of SynCAM 1 transcripts in the visual cortex after monocular deprivation (Lyckman et al., 2008) and in regenerating spinal cord axons (Zelano et al., 2009), two processes that require the formation of new synapses.

Moreover, this study demonstrates that SynCAM 1 not only impacts functional synapse number but also regulates the activity-dependent plasticity of synapses once they are formed. Specifically, SynCAM 1 overexpression occluded LTD and the loss of SynCAM 1 enhanced LTD. Furthermore, mice in which SynCAM 1 overexpression was shut down subsequently again exhibit normal LTD. These findings indicate that the impact of SynCAM 1 on LTD directly depends on its expression level and highlights an unexpected physiological role of this protein. This is the first report that an adhesion molecule can regulate LTD, extending the findings that LTP is affected by NCAM and Eph receptors (Gerrow and El-Husseini, 2006) and that the loss of neuroligin 1 impairs LTP (Blundell et al., 2010; Kim et al., 2008). Two mechanisms underlying the effect of SynCAM 1 on LTD are conceivable. The *trans*-synaptic interaction of SynCAM proteins might stabilize synaptic structures and thereby prevent the physical loss of synaptic contacts that occurs during LTD (Zhou et al., 2004). Also, SynCAM complexes may confine glutamate receptors to postsynaptic specializations, thereby preventing LTD. Future studies will have to test these possibilities.

Perhaps the most surprising finding of this study is that SynCAM 1 is the first adhesion molecule that can restrict a cognitive function, which extends previous molecular analyses of learning (Lee and Silva, 2009). This effect differs from the loss of neuroligin 1, which was reported to impair spatial learning (Blundell et al., 2010). SynCAM 1 may impact spatial learning through altering LTD, which plays roles in object exploration in space and spatial learning (Kemp and Manahan-Vaughan, 2004; Nicholls et al., 2008).

In summary, our studies of SynCAM 1 define for the first time the functions of a synapse-organizing protein during the development of synapses in vivo and show that it can promote both an increase in synapse number and the maintenance thereof, together with regulating plasticity.

EXPERIMENTAL PROCEDURES

Transgenic and KO SynCAM 1 Mouse Models

To generate the transgenic cassette, a SynCAM 1 construct tagged within the middle of the cytosolic sequence with two flag epitopes was cloned into the pTRE vector (Clontech). This coding sequence preceded by a TRE element (Mansuy and Bujard, 2000) was used to generate a transgenic mouse line, which was crossed to mice carrying the CaMKII-tTA transgene (Mayford et al., 1996) to obtain double-heterozygotic SynCAM 1^{flag} overexpressors. To temporally control SynCAM 1^{flag} overexpression, doxycycline-containing water (1 g/l) was provided to the mice. Transgenic mice were maintained in a mixed BL6/SJLF1J background, and mice heterozygotic for the CaMKII-tTA transgene but lacking the SynCAM 1^{flag} transgene served as controls. SynCAM 1 KO mice were generously provided by Dr. T. Momoi (National Institute for Neuroscience, Tokyo) (Fujita et al., 2006). This mouse line was maintained in a mixed BL6/129Sv background and homozygotic wild-type and KO littermates were compared to control for the same genetic background of analyzed mice.

Biochemical Procedures

Frozen tissue samples were rapidly homogenized using microtip-aided sonication. Brain homogenates were subfractionated by the method of Jones and Matus (1974) with modifications (Biederer et al., 2002). For coimmunoprecipitation experiments, synaptosomes were prepared from forebrain, solubilized with 1% Triton X-100, and incubated with Protein G agarose-conjugated flag M2 antibodies or with anti-SynCAM 1 antibodies as described previously (Fogel et al., 2007). Quantitative immunoblotting was performed on an Odyssey Imaging System (Li-Cor, Lincoln, NE) and signals were calibrated against purified epitopes (Fogel et al., 2007).

Immunohistochemistry and Electron Microscopy

Immunohistochemistry was performed on cryosections of P21 mouse brains, and stained sections were imaged with a Zeiss LSM 510 META laser scanning confocal microscope. Golgi staining of hippocampal pyramidal neurons was performed using the FD Rapid Golgi Stain Kit (FD NeuroTechnologies, Ellicott City, MD) according to the manufacturer's instructions. Differential interference contrast images of secondary and tertiary CA1 apical dendrites were acquired and spines of Golgi-stained sections were classified and quantitatively analyzed as described (Knott et al., 2006; Li et al., 2004). For electron microscopy, coronal sections of 100 μm thickness from the CA1 stratum radiatum of hippocampus were cut using a vibratome. Morphometric classification of synapses and analysis of ultrastructural parameters were performed as described (Rosahl et al., 1995).

Electrophysiological Recordings

Electrophysiological recordings from hippocampal slices were performed after preparing 400 μm slices and storing them in artificial cerebrospinal fluid (ACSF) gassed with carbogen. For whole cell recordings, pyramidal CA1 neurons were visualized using differential infrared video microscopy. Miniature EPSCs were recorded at a holding potential of −70 mV in ACSF supplemented with tetrodotoxin, picrotoxin, and trichlormethiazide. Statistical analyses of cumulative distributions were performed applying the Kolmogorov-Smirnov test. Field potentials were evoked by stimulating Schaffer collaterals and recorded in the CA1 stratum radiatum. LTP was induced by two trains of pulses at 100 Hz for 1 s, and LTD by low frequency stimulation of 1 Hz for 15 min.

Behavioral Studies

Behavioral tests were performed using cohorts of male mice. Locomotor activity in an open field box and a water tank was controlled by video tracking. Novel object exploration was scored as described with modifications to test hippocampal effects (Gresack and Frick, 2004). Morris water maze training and probe trials were conducted in a water-filled circular tank, with visual cues mounted on the tank wall. Path length, time spent in each quadrant, and latency to find the escape platform were tracked by video as described (Rabenstein et al., 2005). Elevated plus maze studies were performed by measuring the frequency with which mice enter open and close maze arms as described (Lister, 1987).

Analyses were performed blinded to the genotype. In OE studies, mice carried one SynCAM 1^{flag} and one tTA transgene, while their littermate controls carried only one tTA transgene. In KO studies, wild-type controls refer to homozygous littermates of KO mice.

SUPPLEMENTAL INFORMATION

Supplemental Information includes Supplemental Experimental Procedures, six figures, and one table and can be found with this article online at doi:10.1016/j.neuron.2010.11.003.

ACKNOWLEDGMENTS

We thank Ms Y. Lei, N. Meyer, and A. Gruschka for technical assistance and Drs. S. Chandra, L. Chen, R. Klein, and T. Mrsic-Flogel for discussions and comments on the manuscript. We are grateful to Dr. T. Momoi for generously providing the SynCAM 1/RA175 KO mouse line, Dr. R. Hammer for generating the transgenic line, and Dr. M. Picciotto for support of behavioral studies. We thank M. Graham and Dr. C. Rahner for expert support of our EM studies. E.M.R. performed histochemical and ultrastructural studies, protein expression and interaction analyses, and behavioral experiments, A.J.K. performed electrophysiological analyses, K.P. performed and analyzed ultrastructural studies, A.K.G. performed behavioral studies, A.I.F. quantified protein expression, A.B. initially bred transgenic mice and confirmed expression, T.B. and T.C.S. conceived in collaboration the transgenic approach and T.C.S. supervised A.B., V.S. conceived and supervised the physiological approaches and performed electrophysiological analyses, and T.B. conceived and supervised nonphysiological approaches, performed protein expression and interaction analyses and histochemical studies, and wrote the manuscript. This work was supported by the National Institute of Health Grant R01 DA018928 (to T.B.), a March of Dimes Basil O'Connor Award (to T.B.), and a Scottish Rite Schizophrenia fellowship (to E.M.R).

Accepted: September 17, 2010
Published: December 8, 2010

REFERENCES

Biederer, T. (2006). Bioinformatic characterization of the SynCAM family of immunoglobulin-like domain-containing adhesion molecules. Genomics *87*, 139–150.

Biederer, T., Sara, Y., Mozhayeva, M., Atasoy, D., Liu, X., Kavalali, E.T., and Südhof, T.C. (2002). SynCAM, a synaptic adhesion molecule that drives synapse assembly. Science *297*, 1525–1531.

Biederer, T., and Stagi, M. (2008). Signaling by synaptogenic molecules. Curr. Opin. Neurobiol. *18*, 261–269.

Blundell, J., Blaiss, C.A., Etherton, M.R., Espinosa, F., Tabuchi, K., Walz, C., Bolliger, M.F., Sudhof, T.C., and Powell, C.M. (2010). Neuroligin-1 deletion results in impaired spatial memory and increased repetitive behavior. J. Neurosci. *30*, 2115–2129.

Bourgeron, T. (2009). A synaptic trek to autism. Curr. Opin. Neurobiol. *19*, 231–234.

Cheng, D., Hoogenraad, C.C., Rush, J., Ramm, E., Schlager, M.A., Duong, D.M., Xu, P., Wijayawardana, S.R., Hanfelt, J., Nakagawa, T., et al. (2006). Relative and absolute quantification of postsynaptic density proteome isolated from rat forebrain and cerebellum. Mol. Cell. Proteomics *5*, 1158–1170.

Chih, B., Engelman, H., and Scheiffele, P. (2005). Control of excitatory and inhibitory synapse formation by neuroligins. Science *307*, 1324–1328.

Chubykin, A.A., Atasoy, D., Etherton, M.R., Brose, N., Kavalali, E.T., Gibson, J.R., and Südhof, T.C. (2007). Activity-dependent validation of excitatory versus inhibitory synapses by neuroligin-1 versus neuroligin-2. Neuron *54*, 919–931.

Davis, G.W., Schuster, C.M., and Goodman, C.S. (1997). Genetic analysis of the mechanisms controlling target selection: Target-derived Fasciclin II regulates the pattern of synapse formation. Neuron *19*, 561–573.

Fiala, J.C., Spacek, J., and Harris, K.M. (2002). Dendritic spine pathology: Cause or consequence of neurological disorders? Brain Res. Brain Res. Rev. *39*, 29–54.

Fogel, A.I., Akins, M.R., Krupp, A.J., Stagi, M., Stein, V., and Biederer, T. (2007). SynCAMs organize synapses through heterophilic adhesion. J. Neurosci. *27*, 12516–12530.

Fujita, E., Kouroku, Y., Ozeki, S., Tanabe, Y., Toyama, Y., Maekawa, M., Kojima, N., Senoo, H., Toshimori, K., and Momoi, T. (2006). Oligo-asthenoteratozoospermia in mice lacking RA175/TSLC1/SynCAM/IGSF4A, a cell adhesion molecule in the immunoglobulin superfamily. Mol. Cell. Biol. *26*, 718–726.

Gage, F.H., Dunnett, S.B., and Bjorklund, A. (1989). Age-related impairments in spatial memory are independent of those in sensorimotor skills. Neurobiol. Aging *10*, 347–352.

Gerrow, K., and El-Husseini, A. (2006). Cell adhesion molecules at the synapse. Front. Biosci. *11*, 2400–2419.

Giagtzoglou, N., Ly, C.V., and Bellen, H.J. (2009). Cell adhesion, the backbone of the synapse: "Vertebrate" and "invertebrate" perspectives. Cold Spring Harb. Perspect. Biol. *1*, a003079.

Graf, E.R., Zhang, X., Jin, S.-X., Linhoff, M.W., and Craig, A.M. (2004). Neurexins induce differentiation of GABA and glutamate postsynaptic specializations via neuroligins. Cell *119*, 1013–1026.

Gresack, J.E., and Frick, K.M. (2004). Environmental enrichment reduces the mnemonic and neural benefits of estrogen. Neuroscience *128*, 459–471.

Hung, A.Y., Futai, K., Sala, C., Valtschanoff, J.G., Ryu, J., Woodworth, M.A., Kidd, F.L., Sung, C.C., Miyakawa, T., Bear, M.F., et al. (2008). Smaller dendritic spines, weaker synaptic transmission, but enhanced spatial learning in mice lacking Shank1. J. Neurosci. *28*, 1697–1708.

Irwin, S.A., Patel, B., Idupulapati, M., Harris, J.B., Crisostomo, R.A., Larsen, B.P., Kooy, F., Willems, P.J., Cras, P., Kozlowski, P.B., et al. (2001). Abnormal dendritic spine characteristics in the temporal and visual cortices of patients with fragile-X syndrome: A quantitative examination. Am. J. Med. Genet. *98*, 161–167.

Jin, Y., and Garner, C.C. (2008). Molecular mechanisms of presynaptic differentiation. Annu. Rev. Cell Dev. Biol. *24*, 237–262.

Jones, D.H., and Matus, A.I. (1974). Isolation of synaptic plasma membrane from brain by combined flotation-sedimentation density gradient centrifugation. Biochim. Biophys. Acta *356*, 276–287.

Kayser, M.S., McClelland, A.C., Hughes, E.G., and Dalva, M.B. (2006). Intracellular and trans-synaptic regulation of glutamatergic synaptogenesis by EphB receptors. J. Neurosci. *26*, 12152–12164.

Kemp, A., and Manahan-Vaughan, D. (2004). Hippocampal long-term depression and long-term potentiation encode different aspects of novelty acquisition. Proc. Natl. Acad. Sci. USA *101*, 8192–8197.

Kim, J., Jung, S.Y., Lee, Y.K., Park, S., Choi, J.S., Lee, C.J., Kim, H.S., Choi, Y.B., Scheiffele, P., Bailey, C.H., et al. (2008). Neuroligin-1 is required for normal expression of LTP and associative fear memory in the amygdala of adult animals. Proc. Natl. Acad. Sci. USA *105*, 9087–9092.

Knott, G.W., Holtmaat, A., Wilbrecht, L., Welker, E., and Svoboda, K. (2006). Spine growth precedes synapse formation in the adult neocortex in vivo. Nat. Neurosci. *9*, 1117–1124.

Lee, Y.S., and Silva, A.J. (2009). The molecular and cellular biology of enhanced cognition. Nat. Rev. Neurosci. *10*, 126–140.

Li, C., Brake, W.G., Romeo, R.D., Dunlop, J.C., Gordon, M., Buzescu, R., Magarinos, A.M., Allen, P.B., Greengard, P., Luine, V., and McEwen, B.S. (2004). Estrogen alters hippocampal dendritic spine shape and enhances synaptic protein immunoreactivity and spatial memory in female mice. Proc. Natl. Acad. Sci. USA *101*, 2185–2190.

Lister, R.G. (1987). The use of a plus-maze to measure anxiety in the mouse. Psychopharmacology (Berl.) *92*, 180–185.

Lyckman, A.W., Horng, S., Leamey, C.A., Tropea, D., Watakabe, A., Van Wart, A., McCurry, C., Yamamori, T., and Sur, M. (2008). Gene expression patterns in

visual cortex during the critical period: Synaptic stabilization and reversal by visual deprivation. Proc. Natl. Acad. Sci. USA *105*, 9409–9414.

Mansuy, I.M., and Bujard, H. (2000). Tetracycline-regulated gene expression in the brain. Curr. Opin. Neurobiol. *10*, 593–596.

Mayford, M., Bach, M.E., Huang, Y.Y., Wang, L., Hawkins, R.D., and Kandel, E.R. (1996). Control of memory formation through regulated expression of a CaMKII transgene. Science *274*, 1678–1683.

Megias, M., Emri, Z., Freund, T.F., and Gulyas, A.I. (2001). Total number and distribution of inhibitory and excitatory synapses on hippocampal CA1 pyramidal cells. Neuroscience *102*, 527–540.

Nam, C.I., and Chen, L. (2005). Postsynaptic assembly induced by neurexin-neuroligin interaction and neurotransmitter. Proc. Natl. Acad. Sci. USA *102*, 6137–6142.

Nelson, S.B., and Turrigiano, G.G. (2008). Strength through diversity. Neuron *60*, 477–482.

Neves, G., Cooke, S.F., and Bliss, T.V. (2008). Synaptic plasticity, memory and the hippocampus: A neural network approach to causality. Nat. Rev. Neurosci. *9*, 65–75.

Nicholls, R.E., Alarcon, J.M., Malleret, G., Carroll, R.C., Grody, M., Vronskaya, S., and Kandel, E.R. (2008). Transgenic mice lacking NMDAR-dependent LTD exhibit deficits in behavioral flexibility. Neuron *58*, 104–117.

Okamura, K., Tanaka, H., Yagita, Y., Saeki, Y., Taguchi, A., Hiraoka, Y., Zeng, L.H., Colman, D.R., and Miki, N. (2004). Cadherin activity is required for activity-induced spine remodeling. J. Cell Biol. *167*, 961–972.

Rabenstein, R.L., Addy, N.A., Caldarone, B.J., Asaka, Y., Gruenbaum, L.M., Peters, L.L., Gilligan, D.M., Fitzsimonds, R.M., and Picciotto, M.R. (2005). Impaired synaptic plasticity and learning in mice lacking beta-adducin, an actin-regulating protein. J. Neurosci. *25*, 2138–2145.

Raghavachari, S., and Lisman, J.E. (2004). Properties of quantal transmission at CA1 synapses. J. Neurophysiol. *92*, 2456–2467.

Rosahl, T.W., Spillane, D., Missler, M., Herz, J., Selig, D.K., Wolff, J.R., Hammer, R.E., Malenka, R.C., and Südhof, T.C. (1995). Essential functions of synapsins I and II in synaptic vesicle regulation. Nature *375*, 488–493.

Sara, Y., Biederer, T., Atasoy, D., Chubykin, A., Mozhayeva, M.G., Südhof, T.C., and Kavalali, E.T. (2005). Selective capability of SynCAM and neuroligin for functional synapse assembly. J. Neurosci. *25*, 260–270.

Scheiffele, P., Fan, J., Choih, J., Fetter, R., and Serafini, T. (2000). Neuroligin expressed in nonneuronal cells triggers presynaptic development in contacting axons. Cell *101*, 657–669.

Stagi, M., Fogel, A.I., and Biederer, T. (2010). SynCAM 1 participates in axo-dendritic contact assembly and shapes neuronal growth cones. Proc. Natl. Acad. Sci. USA *107*, 7568–7573.

Südhof, T.C. (2008). Neuroligins and neurexins link synaptic function to cognitive disease. Nature *455*, 903–911.

Thomas, L.A., Akins, M.R., and Biederer, T. (2008). Expression and adhesion profiles of SynCAM molecules indicate distinct neuronal functions. J. Comp. Neurol. *510*, 47–67.

Togashi, H., Abe, K., Mizoguchi, A., Takaoka, K., Chisaka, O., and Takeichi, M. (2002). Cadherin regulates dendritic spine morphogenesis. Neuron *35*, 77–89.

Varoqueaux, F., Aramuni, G., Rawson, R.L., Mohrmann, R., Missler, M., Gottmann, K., Zhang, W., Südhof, T.C., and Brose, N. (2006). Neuroligins determine synapse maturation and function. Neuron *51*, 741–754.

Verhage, M., Maia, A.S., Plomp, J.J., Brussaard, A.B., Heeroma, J.H., Vermeer, H., Toonen, R.F., Hammer, R.E., van den Berg, T.K., Missler, M., et al. (2000). Synaptic assembly of the brain in the absence of neurotransmitter secretion. Science *287*, 864–869.

Wang, K., Zhang, H., Ma, D., Bucan, M., Glessner, J.T., Abrahams, B.S., Salyakina, D., Imielinski, M., Bradfield, J.P., Sleiman, P.M., et al. (2009). Common genetic variants on 5p14.1 associate with autism spectrum disorders. Nature *459*, 528–533.

Wierenga, C.J., Becker, N., and Bonhoeffer, T. (2008). GABAergic synapses are formed without the involvement of dendritic protrusions. Nat. Neurosci. *11*, 1044–1052.

Zelano, J., Berg, A., Thams, S., Hailer, N.P., and Cullheim, S. (2009). SynCAM1 expression correlates with restoration of central synapses on spinal motoneurons after two different models of peripheral nerve injury. J. Comp. Neurol. *517*, 670–682.

Zhiling, Y., Fujita, E., Tanabe, Y., Yamagata, T., Momoi, T., and Momoi, M.Y. (2008). Mutations in the gene encoding CADM1 are associated with autism spectrum disorder. Biochem. Biophys. Res. Commun. *377*, 926–929.

Zhou, Q., Homma, K.J., and Poo, M.M. (2004). Shrinkage of dendritic spines associated with long-term depression of hippocampal synapses. Neuron *44*, 749–757.

Ziv, N.E., and Smith, S.J. (1996). Evidence for a role of dendritic filopodia in synaptogenesis and spine formation. Neuron *17*, 91–102.

Zoghbi, H.Y. (2003). Postnatal neurodevelopmental disorders: Meeting at the synapse? Science *302*, 826–830.

Neuron, Volume 68

Supplemental Information

SynCAM 1 Adhesion Dynamically Regulates Synapse Number and Impacts Plasticity and Learning

Elissa M. Robbins, Alexander J. Krupp, Karen Perez de Arce, Ananda K. Ghosh, Adam I. Fogel, Antony Boucard, Thomas C. Südhof, Valentin Stein, and Thomas Biederer

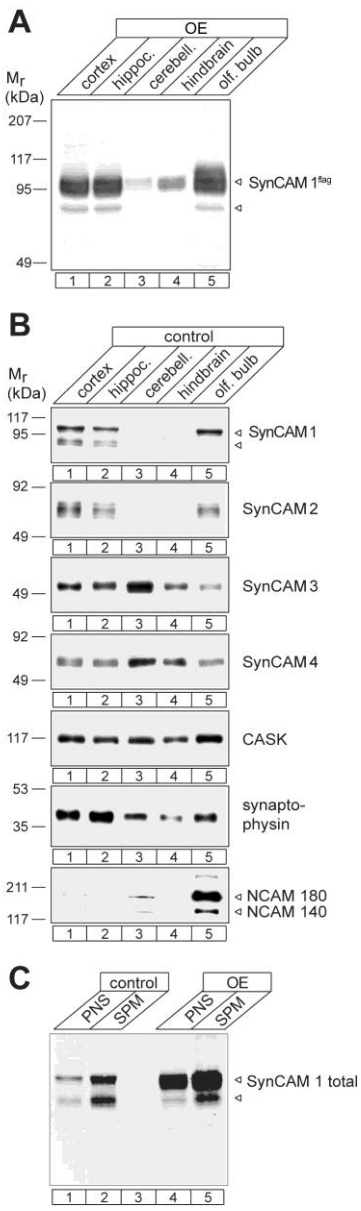

Figure S1, related to Figure 1. Forebrain Overexpression of Transgenic SynCAM 1^{flag} Protein.
(A and B) Brain regions were prepared from transgenic overexpressor (OE) and control mice at 10 weeks of age. Equal amounts of 20 µg were analyzed by immunoblotting as indicated. Both SynCAM 1^{flag} and endogenous SynCAM 1 are predominantly expressed in forebrain. (A) Expression of SynCAM 1^{flag} protein in brain regions of transgenic OE detected with anti-flag antibodies. Note that the overexpressed protein has the same apparent molecular weight of 100 kDa with a lower molecular weight fraction as the endogenous SynCAM 1, consistent with the correct glycosylation of its extracellular domain. (B) Endogenous expression of SynCAM 1 and SynCAM 2 is highest in forebrain, whereas SynCAM 3 and SynCAM 4 are expressed throughout the brain, with highest levels in cerebellum. Note that SynCAM 2 can appear heterogenous depending on the sample preparation due to its complex N-glycosylation pattern. (C) Synaptic plasma membranes (SPM) were prepared from tTA control mice and transgenic OE at 10 weeks of age and analyzed by quantitative immunoblotting with specific antibodies detecting SynCAM 1. SynCAM 1 is strongly enriched in the SPM fraction of both tTA control and overexpressing mice. PNS, postnuclear supernatant.

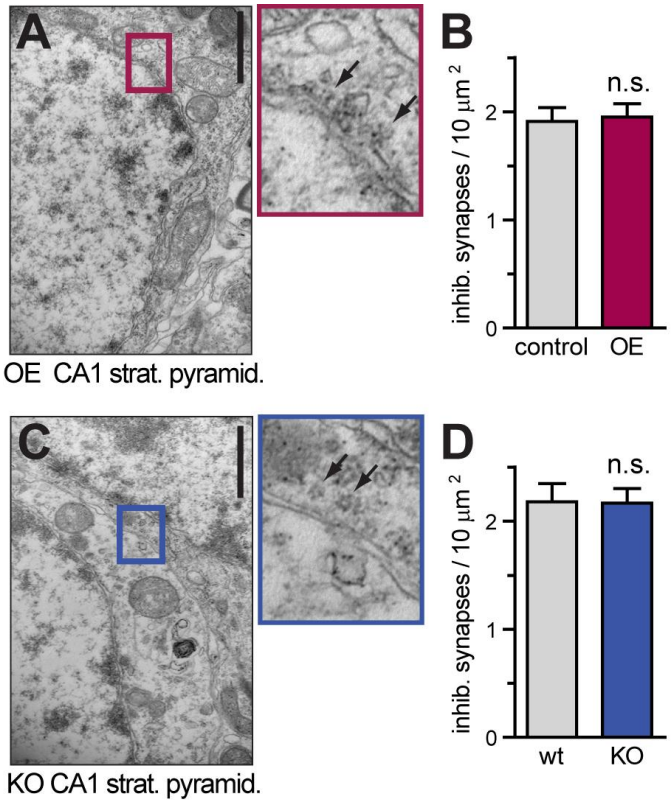

Figure S2, related to Figure 2. Inhibitory Perisomal Synapses are Unaffected by SynCAM 1.
Inhibitory synapse numbers in CA1 stratum pyramidale are unaffected by either SynCAM 1 overexpression (A, B) or KO (C, D). Representative electron micrographs of inhibitory perisomal synapses are shown on the left in (A, C) (magnification 26,500x). The enlarged images depict the perisomal synapse boxed in these micrographs, with arrows pointing to synaptic vesicles. Scale bars, 1 µm. (B, D) Quantification of data in (A, C). (tTA controls, n=60 images, 179 synapses, 3 male littermates; OE, n=60 images, 183 synapses, 3 males; wild-type, n=40 images, 136 synapses, 2 male littermates; KO, n=60 images, 203 synapses, 3 male mice.)

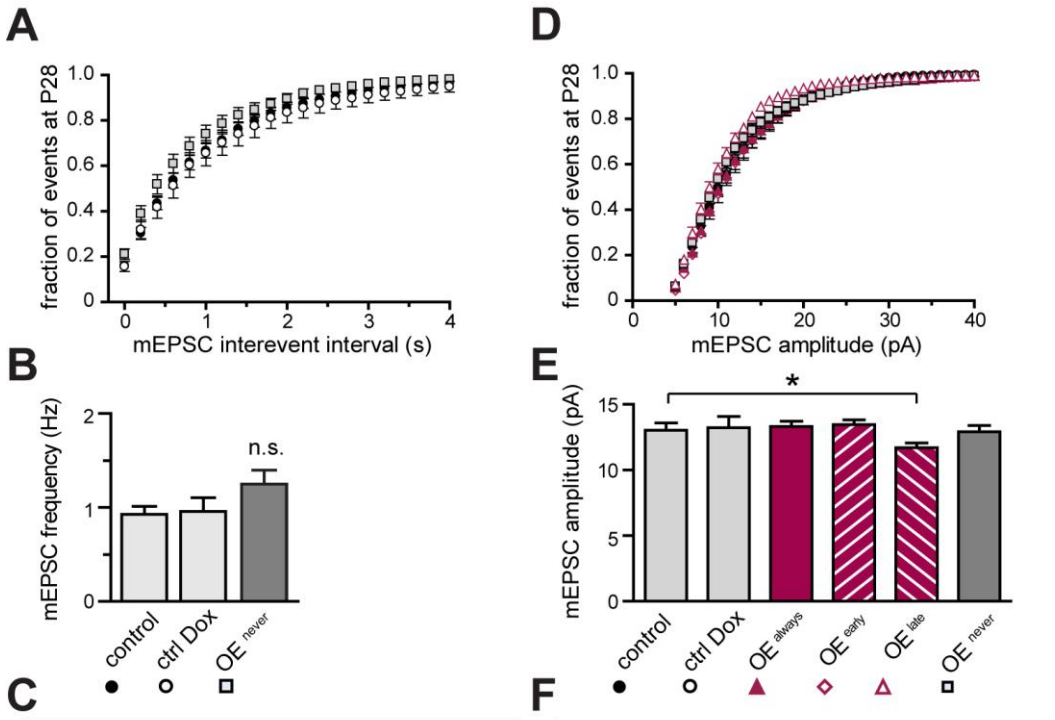

intervals	OE^{always}	OE^{late}	OE^{early}	OE^{never}	ctrl Dox
OE^{late}	1				
OE^{early}	0.001	0.001			
OE^{never}	0.001	0.001	1		
ctrl Dox	0.001	0.001	1	1	
ctrl tTA	0.001	0.001	1	1	1

amplitudes	OE^{always}	OE^{late}	OE^{early}	OE^{never}	ctrl Dox
OE^{late}	1				
OE^{early}	1	0.025			
OE^{never}	1	1	0.1		
ctrl Dox	1	1	1	1	
ctrl tTA	1	0.01	1	0.05	0.1

Figure S3, related to Figure 5. Physiological Controls of Conditional SynCAM 1^{flag} Overexpression.
(A) Cumulative distribution of mEPSC interevent intervals at P28. Doxycycline efficiently represses the increased mEPSC frequencies in SynCAM 1^{flag} overexpressors. For symbol legends, see panel (B).
(B) Mean mEPSC frequencies of the conditions shown in (A). Miniature EPSC frequencies of untreated tTA control littermates (control) are indistinguishable from those of continuously repressed mice (OE^{never}). (tTA controls 0.9 ± 0.1 Hz, n=11; OE^{never} 1.3 ± 0.1 Hz, n=12) Doxycycline treatment of animals that only carry the tTA transgene (ctrl Dox) has no effect on mEPSC frequencies (1.0 ± 0.1 Hz, n=8). n.s., not significant.
(C) Cumulative distributions of mEPSC interevent intervals were tested for significance using the Kolmogorov-Smirnov (KS) test. KS p values are stated in the table, with a significance level of 0.01.
(D) Cumulative distributions of mEPSC amplitudes at P28 were indistinguishable between most SynCAM 1^{flag} expression conditions. Only after late SynCAM 1^{flag} expression (OE^{late}), mEPSC amplitudes were slightly decreased compared to all other conditions. For symbol legends, see panel (E).
(E) Mean mEPSC amplitudes of the conditions shown in (D). (OE^{late} 11.7 ± 0.4 pA, n=7; OE^{always} 13.3 ± 0.4 pA, n=8; OE^{early} 13.5 ± 0.4 pA, n=11; OE^{never} 12.9 ± 0.5 pA, n=12; tTA control 13.0 ± 0.5 pA, n=11; ctrl Dox 13.2 ± 0.9 pA, n=8) Note that the slight reduction in mEPSC amplitude of OE^{late} was only significantly different from tTA controls, but not when compared to the other conditions. This could be due to the high sensitivity of the Kolmogorov-Smirnov test used to test for statistical difference of mEPSC distributions.
(F) Cumulative distributions of mEPSC amplitudes were tested for significance using the Kolmogorov-Smirnov (KS) test. KS p values are stated in the table. Significance level for the KS test was 0.01.

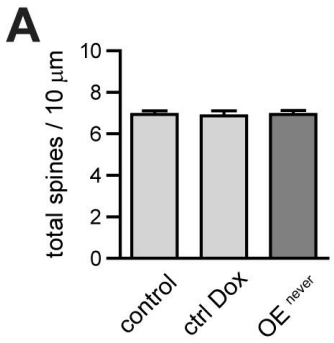

B

		spines	n males
OE	P14	593	2
tTA ctrl	P14	551	2
OE^{always}	P28	1022	3
OE^{early}	P28	764	3
OE^{late}	P28	743	3
OE^{never}	P28	467	2
tTA ctrl	P28	784	2
tTA Dox	P28	446	2

Figure S4, related to Figure 5. Morphological Controls of Conditional SynCAM 1^{flag} Overexpression.
(A) At P28, spine densities of untreated tTA control littermates (control) measured after Golgi staining are indistinguishable from those of continuously repressed mice (OE^{never}). Doxycycline treatment of animals that only carry the tTA transgene (ctrl Dox) has no effect on spine densities.
(B) Statistical information for morphological control experiments shown in (A) and Figure 5E.

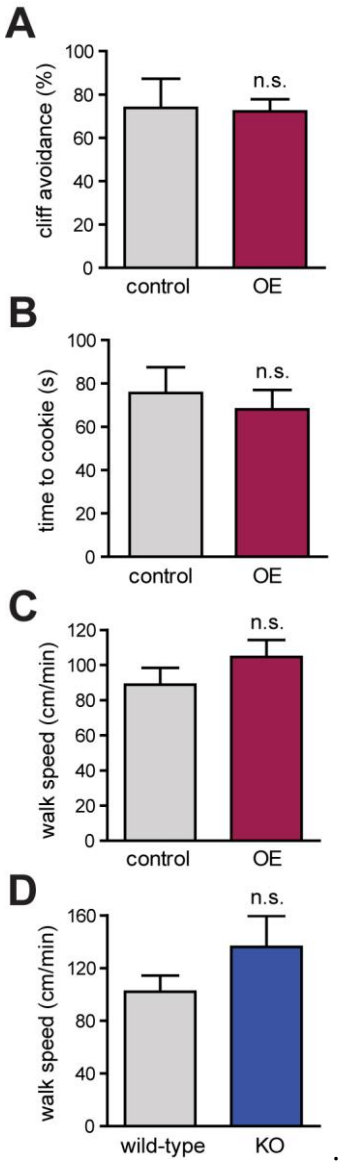

Figure S5, related to Figure 7. Sensory and Motor Controls in SynCAM 1^{flag} Overexpressors and KO Mice.

(A) Visual acuity, measured by performance in the visual cliff task, is not altered in SynCAM 1^{flag} overexpressing animals. Results in (A, B) were obtained from 9 tTA littermate control and 9 SynCAM 1 OE male mice at 3-5 months. n.s., not significant.

(B) Olfactory discrimination, measured by performance in the hidden cookie task, is not altered in SynCAM 1^{flag} overexpressing animals.

(C) Locomotor activity, measured as walk speed calculated from total distance traveled in an open field over 20 min, is not altered in SynCAM 1^{flag} overexpressing animals. Results were obtained from 11 tTA littermate control and 12 SynCAM 1 OE male mice at 3-5 months.

(D) Walk speed in an open field is not altered in SynCAM 1 KO animals. Results were obtained from 8 wild-type littermate control and 9 SynCAM 1 KO male mice at 6-12 months.

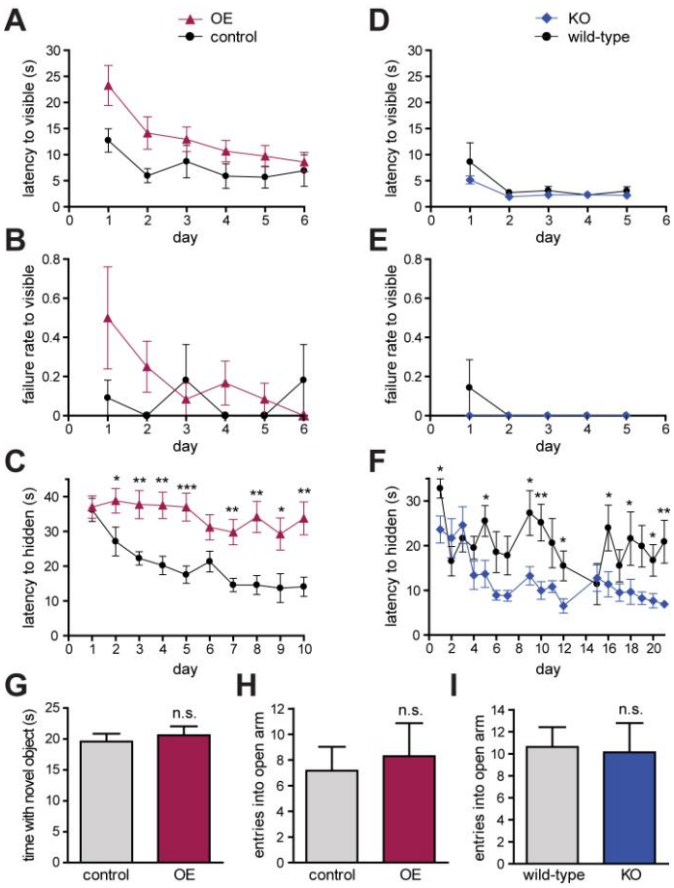

Figure S6, related to Figure 7. Behavioral Controls of SynCAM 1^{flag} Overexpressors and KO Mice.
(A and B) SynCAM 1 transgenic mice (red triangles) locate a visible platform in the Morris water maze indistinguishably from littermate controls (black circles), indicating that visual acuity (A) and motivation (B) are unaltered in these animals. Results in (A-C) were obtained from 11 tTA littermate controls and 12 SynCAM 1 OE male mice at 4-5 months.
(C) Spatial reference learning is strongly impaired in SynCAM 1 overexpressors. Controls (black circles) learn over daily trials in the Morris water maze to locate the hidden escape platform, whereas SynCAM 1 overexpressors (red triangles) fail to learn as measured by the latency to the platform. Note that animals were 4-5 months of age, in contrast to the aged mice analyzed for the KO studies in (F).
(D and E) SynCAM 1 KO mice (blue diamonds) locate a visible platform in the Morris water maze to the same extent as wild type littermate controls (black circles), demonstrating unaltered visual acuity (D) and motivation (E). Results in (D-F) were obtained from 7 wild-type littermate controls and 9 SynCAM 1 KO male mice at 6-12 months.
(F) SynCAM 1 KO mice (blue diamonds) exhibit improved spatial learning compared to wild-type littermates (black circles). Learning ability was intentionally compromised by analyzing aged mice at 6-12 months, resulting in the observed prolonged latencies in wild types. Extended training was performed to allow these aged wild-type controls to learn the task.
(G) SynCAM 1^{flag} overexpressors show no learning difference in the novel object recognition paradigm. Results were obtained from 9 wild-type littermate control and 9 SynCAM 1 KO male mice at 3-5 months. n.s., not significant.
(H and I) SynCAM 1^{flag} transgenic overexpressor (H) and KO mice (I) do not show significant differences in the number of open arm entries when compared to their respective controls. Results in (H) were obtained from 11 tTA littermate controls and 12 SynCAM 1 OE male mice at 3-4 months, and in (I) from 8 wild-type littermate controls and 9 SynCAM 1 KO male mice at 6-12 months.

A

	rat forebrain	SPM enrichment
SynCAM 1	0.15 ng/µg	2.8
SynCAM 2	1.2 ng/µg	3.3
SynCAM 3	0.27 ng/µg	1.8
SynCAM 4	0.04 ng/µg	4.5

B

	hippocampus	cortex	cerebellum
SynCAM 1	0.08 ng/µg	0.14 ng/µg	0.02 ng/µg
SynCAM 2	0.52 ng/µg	0.92 ng/µg	0.23 ng/µg
SynCAM 3	0.13 ng/µg	0.25 ng/µg	0.46 ng/µg
SynCAM 4	0.05 ng/µg	0.07 ng/µg	0.14 ng/µg

Table S1. SynCAMs are Abundant Brain Proteins.
(A) SynCAM protein expression in rat forebrain homogenate at P9. For analysis of purified synaptic plasma membranes (SPM), see the Main Text. Quantitative immunoblotting was performed using previously reported antibodies and purified epitopes comprised of extracellular domains and intracellular sequences (Fogel et al., 2007).
(B) SynCAM protein expression in homogenates of the indicated rat brain regions at P28. SynCAM 1 and 2 are most prominent in forebrain regions, while SynCAM 3 is abundant in cerebellum (Thomas et al., 2008). Detection was performed as described in (A).

SUPPLEMENTAL EXPERIMENTAL PROCEDURES

Antibodies. Immunoblotting was performed with specific antibodies against SynCAM 1 (YUC8. 1:1000), SynCAM 2 (YU524, 1:1000), SynCAM 3 (YU525, 1:1000), and SynCAM 4 (YU591, 1:1000) that were described previously and detect these proteins at apparent molecular weights of 100 kDa, 62-76 kDa, 49 kDa, and 67 kDa, respectively (Fogel et al., 2007). Apparent molecular weights of all SynCAM proteins are higher than predicted from the open reading frames due to N-glycosylation (Fogel et al., 2007). For simultaneous detection of SynCAMs 1-3, we utilized a pleioSynCAM antibody (T2412, 1:2000) raised in rabbits against the SynCAM 1 carboxyl-terminal sequence that recognizes this conserved sequence in SynCAM 1, 2 and 3, but not 4 (Fogel et al., 2007). Antibodies to flag (clone M2, F1804; 1:2000) were obtained from Sigma-Aldrich (St. Louis, MO, USA), to N-cadherin from BD Biosciences (San Jose, CA, USA; 1:2000), to NCAM from Sigma-Aldrich (clone OB11; 1:400), to EphB2 from Santa Cruz (Santa Cruz, CA, USA; sc-1763, 1:1000), to CASK (clone K56A/50, 1:1000) and neuroligin 1 (clone N97A/31, 1:1000) from NeuroMab (UC Davis, CA, USA), and to synaptophysin (clone 7.2; 1:10,000) from Synaptic Systems (Göttingen, Germany). Monoclonal antibodies to actin (clone JLA20, developed by Jim Jung-Ching Lin) were obtained from the Developmental Studies Hybridoma Bank maintained by the University of Iowa and used for immunoblotting at 1:100.

For immunolocalization in brain sections, antibodies were employed against flag (M2, 1:2000), the synaptic markers vGlut1 (Millipore AB5905) and vGlut2 (Millipore AB5907) (applied in combination at each 1:1000), and GAD65 (Millipore AB5082, 1:1000).

Transgenic mouse generation. To generate the transgenic cassette, the pTRE vector (Clontech) was modified after filling in the unqiue XhoI site to generate a new PvuI site, and the coding sequence for mouse SynCAM 1 was subcloned from pCMV3333644 (Biederer et al., 2002) after EcoRI digest and filling in into the XbaI site of the modified pTRE. A NheI site was generated using the PCR mutagenesis kit (Stratagene) to generate pTRE mSynCAM1(420)*NheI, with the bracketed number indicating the

amino acid into whose codon the restriction site was introduced. A cassette of two flag epitopes flanking a central tetracysteine motif was inserted into this NheI site using the annealed oligos TMA02183 (ctagcgctgactacaaggacgacgatgacaaatgctgtccaggatgctgtgactacaaggacgacgatgacaagcttg) / TMA02184 (ctagcaagcttgtcatcgtcgtccttgtagtcacagcatcctggacagcatttgtcatcgtcgtccttgtagtcagcg). This inserted the flag-epitope containing cassette in the middle of the cytosolic SynCAM 1 sequence to facilitate the immunohistochemical detection and biochemical purification of the transgenic SynCAM 1^{flag} while minimally interfering with its intracellular protein interaction motifs (Biederer, 2006). The resulting pTRE mSynCAM1(420)flagC_4flag vector was digested with PvuI/NgoMIV to obtain a 2.88 kb fragment including the TRE and coding sequences that was injected into BL6SJLF1/J ES cells. The founder of the transgenic line reported here had 5 copies of the transgene inserted. These transgenic x TRE-SynCAM 1^{flag} +/- mice were crossed to mice overexpressing the transcriptional transactivator tTA from a CaMKII promoter (Mayford et al., 1996). All experiments except for electrophysiological analyses were performed on CaMKII-tTA +/- x TRE-SynCAM 1^{flag} +/- mice maintained in this BL6SJLF1/J background. For electrophysiological recordings of littermates, transgenic males were backcrossed to C57/BL6 females for at least 4 generations to obtain offspring. Non-overexpressing littermates carrying only the CaMKII-tTA +/- transgene while being TRE-SynCAM 1^{flag} -/- served as controls in this study. Where indicated, CaMKII-tTA +/- x TRE-SynCAM 1^{flag} +/- mice treated with the tTA inhibitor doxycycline served as an additional control. All analyses were performed with littermates to control for their genetic background.

SynCAM 1 KO mouse model. SynCAM 1 KO mice were reported previously (Fujita et al., 2006) and have a mixed BL6/129Sv genetic background. All analyses were performed only with littermates to control for their genetic background.

Animal breeding. Mice were group-housed with a 12 hour light-dark cycle with constant temperature. To suppress SynCAM 1-flag overexpression, 1 g/l doxycycline hyclate (Sigma, and Fargon, Barsbüttel,

Germany) and 5 g/l sucrose (Merck) were added to the drinking water of pregnant mice 14 days after conception. To temporally control SynCAM 1 overexpression, the drinking water was changed to doxycycline-containing or doxycycline-free water at P8 (for LTD experiments) or P14 (for mEPSC recordings) as described in the respective experiments. In LTD experiments, this change from doxycycline-containing to doxycycline-free water was performed earlier than for mEPSC recordings as LTD is best recorded in the third postnatal week. Doxycycline-containing water was protected from light and replaced every 2-3 days to account for the potential instability of the drug.

Sample preparation and biochemical procedures. For preparation of brain tissue, animals were anesthetized with isoflurane (Baxter) and decapitated. The brain was removed from the skull and chilled in phosphate buffered saline (PBS, 4°C). To obtain tissue samples, brain regions were dissected quickly and immediately frozen in liquid nitrogen. Frozen tissue samples were rapidly homogenized using microtip-aided sonication in Hepes pH 7.4 (50 mM), urea (8.0 M), and PMSF (0.5 mM). For preparation of subcellular fractions, fresh brain homogenates were subfractionated by the method of Jones and Matus (Jones and Matus, 1974) with modifications (Biederer et al., 2002). For co-immunoprecipitation experiments, synaptosomes were prepared (Biederer et al., 2002) and solubilized on ice by dounce homogenization in 1% Triton X-100 (Roche) in a homogenization buffer composed of Hepes pH 7.4 (25 mM), KAc (125 mM), and sucrose (320 mM), followed by centrifugation. After preclearing of solubilized synaptosome extracts against unconjugated beads, detergent extracts from overexpressors or controls were incubated overnight with flag M2 antibodies (1:160) or SynCAM 1 antibodies (MBL International, Nagoya, Japan; clone 3E1, 1:300). Antibodies were collected on beads for 1 h, beads were washed 3 times with extraction buffer, and eluted with SDS sample buffer for immunoblotting analysis. Protein concentrations were determined using the Pierce BCA assay. SDS-polyacrylamide gel electrophoresis and immunoblotting were performed using standard procedures. For quantitative immunoblotting, an Odyssey Imaging System (Li-Cor, Lincoln, NE, USA) was used and signals were calibrated against known amounts of purified epitopes (Fogel et al., 2007).

Immunohistochemistry. Immunohistochemistry was performed on 40 µm cryosections prepared from P21 mouse brains. Prior to sacrifice, mice were administered isoflurane and perfused transcardially with cold PBS and 4% PFA. Brains were removed and postfixed overnight in 4% PFA, then cryoprotected in 30% sucrose in PBS. Sections were washed in PBS and permeabilized and blocked in a PBS solution containing 3% normal goat serum and 0.3% Triton-X for 1 hour at room temperature. Primary antibody incubation was performed in the permeabilization/blocking buffer at RT overnight, and detected using suitable Alexa dye-conjugated fluorescent secondary antibodies (Invitrogen, 1:1000). Stained sections were imaged at 10x with an epifluorescence (Nikon Eclipse TE2000-U), or at 63x with a laser scanning confocal microscope (Zeiss LSM 510 META), using the LSM software package with channels scanned separately to avoid signal contamination and a pinhole set to 1 µm for each channel.

Golgi staining. Golgi staining of hippocampal pyramidal neurons was performed using the FD Rapid Golgi Stain Kit (FD NeuroTechnologies, Ellicott City, MD) according to the manufacturer's instructions. Briefly, freshly dissected brains were incubated in the impregnation solution for 3 days at room temperature in the dark. Brains were vibratome sectioned to 100 µm thickness, developed, and permanently mounted. Differential interference contrast images of secondary and tertiary CA1 apical dendrites were acquired at 63x. CA1 dendrites and spines of Golgi-stained sections were quantitatively analyzed as described (Li et al., 2004). Spines were classified as described (Knott et al., 2006) as mushroom spines with head diameters that are much greater than their neck diameters, thin spines that have lengths much larger than their diameters and similar diameters of both head and neck, stubby spines that are short and have similar diameters of both head and neck, and undefined protrusions.

Electron microscopy. Mice were perfused with 10 mM HEPES buffer followed by fixation with 2.5% glutaraldehyde (GA)/2% paraformaldehyde (PFA) in 0.1 M sodium cacodylate. Coronal sections of 100 µm thickness from the CA1 stratum radiatum of hippocampus were cut using a vibratome. Blocks from

these sections were prepared for electron microscopy. Approximately 1000 μm^2 of CA1 stratum radiatum from each sample was imaged by random sampling. Synapse quantifications were compared using the Mann-Whitney statistical test. Morphometric classification of synapses and analysis of ultrastructural parameters were performed as described (Colonnier, 1968; Gray, 1959; Rosahl et al., 1995). Quantifications were performed blind to the genotype. Only littermates were analyzed to control for genetic background,

Slice preparation for electrophysiological recordings.

P14-P19 animals: Animals were anesthetized with Isoflurane (Baxter) and decapitated. The brain was removed from the skull and chilled for 1 min in cooled (4°C) artificial cerebrospinal fluid (ACSF) containing in mM: 125 NaCl; 2.6 KCl; 1.4 $MgSO_4$; 2.5 $CaCl_2$; 1.1 NaH_2PO_4; 27.5 $NaHCO_3$ and 11.1 D-glucose; pH 7.2, 310 mosm/kg. The hippocampus was transversally cut in 400 µm slices (VT1200S, Leica). Slices were equilibrated in a custom made submerged chamber in ACSF continuously gassed with carbogen (95% O_2; 5% CO_2) for 30 min at 32°C, and subsequently kept at RT.

P27-P29 animals: Animals were anesthetized with isoflurane (Baxter) and decapitated. The brain was removed from the skull and chilled for 4 min in sucrose-supplemented artificial cerebrospinal fluid (sucrose-ACSF) containing in mM: 87 NaCl; 26 $NaHCO_3$; 75 sucrose; 25 glucose; 2.5 KCl; 1.25 NaH_2PO_4; 7 $MgCl_2$. 400 µm horizontal slices of the entire brain were prepared in ice-cold sucrose-ACSF using a VT1200S vibratome (Leica). Slices were kept in a custom made interphase chamber in ACSF continuously gassed with carbogen at RT.

Electrophysiological field potential recordings were obtained from P15 – P19 animals. To avert recurrent excitation, Schaffer collaterals were severed between CA3 and CA1. Synaptic responses were evoked by stimulating the Schaffer collaterals at 0.03-0.1 Hz with 0.2 ms pulses. Field EPSPs (fEPSPs) were recorded in the stratum radiatum of the CA1 region using glass microelectrodes (Science Products, Hofheim, Germany) filled with ACSF. Data was acquired using a Multiclamp 700B amplifier (Axon

Instruments) and digitized on a Digidata 1322A (Axon Instruments) and stored on a PC. All experiments were performed at room temperature (22–24°C). fEPSP slopes were used as a measure of dendritic activity and determined between 20-80% of the maximum field amplitude. fEPSP slopes acquired over 2 min were averaged.

For long-term potentiation (LTP) recordings, baseline recordings were obtained for 20 min. LTP was induced by two trains of 0.2 ms pulses at 100 Hz for 1 s with an intertrain interval of 20 s. Post-induction responses were monitored for 60 min.

For long-term depression (LTD) recordings, baseline recordings were obtained for 20 min. LTD was induced by low-frequency stimulation (1 Hz for 15 min). Post-induction responses were monitored for 60 min. Stimulus artifacts are omitted for clarity in sample traces of LTP and LTD.

Whole-cell recordings. Pyramidal CA1 neurons were visualized using differential infrared video microscopy (BX51, Olympus). Slices were constantly superfused with gassed ACSF. Miniature EPSCs were obtained from P14 – P15 or P27 – P29 animals. Evoked EPSCs were obtained from P15 – P19 animals. Recording electrodes had a resistance of 3 - 5 MΩ pulled from borosilicate glass (Science Products, Hofheim, Germany). Internal solution contained (in mM): 150 CsGluconate, 8 NaCl, 2 MgATP, 10 HEPES, 0.2 EGTA, and 5 QX-314 ([2-[(2,6-dimethylphenyl)amino]-2-oxoethyl]-triethylazanium bromide), pH 7.2, 290 mosm/kg. EPSCs were evoked with glass electrodes filled with ACSF. AMPA EPSCs were recorded at -70 mV, the NMDA component was recorded at +40 mV. The NMDA component was taken 70 ms after the stimulus.

Paired-pulse facilitation (PPF) was determined as the ratio of the peak of the second AMPA EPSC to the first peak at an interstimulus interval of 40 ms.

Miniature EPSCs were recorded in voltage clamp at -70 mV in ACSF perfusion (in mM: 125 NaCl; 2.6 KCl; 1.4 $MgSO_4$; 4 $CaCl_2$; 2.7 $MgCl_2$; 1.1 NaH_2PO_4; 27.5 $NaHCO_3$ and 11.1 D-glucose) supplemented with tetrodotoxin (TTX, 0.2 μM), picrotoxin (PTX, 100 μM), and trichlormethiazide

(TCM, 250 μM) to increase mEPSC frequency. mEPSCs were detected off-line and statistically analyzed with a custom written Matlab routine (MathWorks).

Behavioral studies. The series of behavioral tests was performed using cohorts of male mice, with animals first subjected to the open field test followed by the novel object recognition test, the Morris water maze, and finally the elevated plus maze. Different cohorts were tested for visual cliff avoidance and the hidden cookie finding task.

Sensory and motor controls. To assess vision, visual cliff avoidance was performed by placing adult male mice into the visual cliff apparatus suspended by their tails headfirst so that front paws were first to be placed on the elevated beam (n=9 littermate tTA controls and n=9 transgenic overexpressors, aged 3-5 months; 6 trials total). Direction of entry was alternated between trials to correct for possible left-right bias. To record latency, time was started when all four paws contacted the beam and stopped when mice stepped onto either solid flooring (score = 1) or the "visual cliff" (score = 0). Mice that did not choose a side within 5 min were excluded from further testing (1 of 9 controls). Choice scores and latency to choice were compared across genotypes with t-tests. To test for proper olfaction, adult male mice were subjected to a hidden cookie test (n=11 littermate tTA controls and n=12 transgenic overexpressors, aged 11-12 months). Prior to testing, subjects were food deprived overnight. A 1 cm x 1 cm x 0.5 cm cookie cube colored similar to the bedding was hidden under corncob bedding in one corner of a clean mouse cage. Subjects were placed in the center of the cage and latency to finding the hidden cookie was recorded, as defined by making nasal or oral contact. Mice that did not find the cookie within 5 min were excluded from further testing (2 of 11 controls). Latency to cookie finding was analyzed by genotype with t-tests. Locomotor activity was measured in an open field using automated tracking software (Panlab SMART). Mice were placed in a 50 cm x 50 cm x 20 cm plexiglas enclosure with opaque walls and allowed to explore it freely for 20 min. Walk speed was measured by the tracking software and analyzed by genotype with t-tests. Distance traveled during the 20 min duration was binned in 5 min intervals and

habituation to the open field environment was analyzed by genotype with t-tests. Swim speed was obtained during the Morris water maze training as described below using the same tracking software.

Novel object recognition. Object recognition tests were conducted in a lit, quiet room on adult male mice (n=11 littermate tTA controls and n=12 transgenic overexpressors, aged 3-4 months), adapting a described protocol (Gresack and Frick, 2004). Briefly, subjects were allowed 10 min of exploration in an empty cage (45 cm x 24 cm x 20 cm) cleaned with a 70% ethanol for initial habituation. The next day, individual mice were reintroduced to this cage into which two identical objects (50 ml Falcon tubes) had been placed at opposite ends. Mice explored the objects and were returned to their home cages after each had explored the objects for a total of 30 sec. Total time required to accumulate 30 sec exploration was also scored; mice that did not explore the objects for a total of 30 s within 10 min were excluded from further testing (1 of 12 transgenic overexpressors). A choice test was conducted 48 h later, during which one familiar object and one novel object (wrapped 1 ml syringe barrel) were placed at opposite ends of the same cage. The location of the novel object was counter-balanced across mice in each group. Mice were videotaped with a camera mounted above the cage. Exploration was defined as nasal or oral contact with the object, and all sessions were conducted during the light cycle and scored by a single rater. Animal order was counter-balanced across genotypes. Exploration time of the familiar objects in the sample and choice phase was analyzed with t-tests by genotype to verify the absence of side preferences that could bias performance in the following choice phase. Exploration time of the novel object was also analyzed with t-tests by genotype.

Morris water maze training and probe trial. Morris water maze studies were performed as described (Rabenstein et al., 2005). Adult male mice received four training trials per day during their light cycle for 10 days (n=11 littermate tTA controls and n=12 transgenic overexpressors, aged 4-5 months) or 20 days (n=8 wild-type littermate controls and n=9 KO mice, aged 6-12 months). KO and respective control animals were aged to facilitate the detection of learning improvements as described in the results. Animals were tested in a water-filled circular white plastic tank (diameter 100 cm, water temperature 21-22°C). A clear plastic platform (10 cm x 10 cm) was submerged 0.5 cm under water and placed in the

same location in the tank over the training days. For analysis, the tank was divided into four equal quadrants, with animals starting one training trial in each quadrant on all training days. The order of starting quadrants was randomized, and mice were placed facing the tank's edge. Salient visual cues of different shape and color were mounted on the tank wall. Path length, time spent in each quadrant, and latency to find the platform were measured by a SMART video tracking system (San Diego Instruments, San Diego, CA). Animals that did not find the platform within 60 sec were manually placed onto the platform. All animals were allowed to remain on the platform for 15 sec. The intertrial interval was 5 min. On day 11 (transgenic overexpressor and control cohorts) or day 21 (aged KO and control cohorts), the probe trial was performed. The platform was removed, and the mice were placed in the middle of the tank and allowed to swim for 60 sec. Time spent in each quadrant was recorded. On day 12 or 22, respectively, the platform was moved to a different quadrant and marked with a flag. Training in the visible platform task was the same as in the hidden platform procedure, and was performed over 6 consecutive days (transgenic and control cohorts) or 5 days (KO and control cohorts) with the marked platform being moved to a new quadrant at each day of training. Failure rates were calculated based on the number of times animals failed to reach the platform in a time span of 60 seconds. Statistical analysis of swim-time data was performed using two-way ANOVA for repeated measures.

Elevated plus maze. Elevated plus maze studies were performed as described (Lister, 1987). Briefly, adult male overexpressors (n=11 littermate tTA controls and n=12 transgenic overexpressors, aged 3-4 months) or KO (n=8 wild-type littermate controls, n=9 KO mice, aged 6-12 months) entered the intersection of the maze arms facing a closed arm and were allowed 5 minutes to explore. An observer blind to genotype scored entries into open and closed arms. Open arm entries were scored when all four paws crossed into the arm. The time spent and distance traveled in the open versus closed arms was recorded using Panlab SMART tracking software.

Data and Statistical Analysis. Data analysis was performed using GraphPad Prism 5 (Graph Pad Software, La Jolla, USA) and Matlab (Mathworks). Miniature EPSCs were detected using a threshold

algorithm generated in Matlab. Statistical significance was assessed using Student's t-test, the Mann-Whitney test, or the Kolmogorov-Smirnov test at the given significance level (p). Statistical errors stated in the text and figure legends and presented as error bars in the figures correspond to the standard error of mean unless indicated otherwise.

All animal procedures undertaken in this study were approved by the Yale University Institutional Animal Care and Use Committee and were in compliance with governmental regulations by the Regierung von Oberbayern (for V.S.) and NIH guidelines (for T.B.).

SUPPLEMENTAL REFERENCES

Biederer, T. (2006). Bioinformatic characterization of the SynCAM family of immunoglobulin-like domain-containing adhesion molecules. Genomics *87*, 139-150.

Biederer, T., Sara, Y., Mozhayeva, M., Atasoy, D., Liu, X., Kavalali, E.T., and Südhof, T.C. (2002). SynCAM, a synaptic adhesion molecule that drives synapse assembly. Science *297*, 1525-1531.

Colonnier, M. (1968). Synaptic patterns on different cell types in the different laminae of the cat visual cortex. An electron microscope study. Brain Research *9*, 268-287.

Fogel, A.I., Akins, M.R., Krupp, A.J., Stagi, M., Stein, V., and Biederer, T. (2007). SynCAMs organize synapses through heterophilic adhesion. J Neurosci *27*, 12516-12530.

Fujita, E., Kouroku, Y., Ozeki, S., Tanabe, Y., Toyama, Y., Maekawa, M., Kojima, N., Senoo, H., Toshimori, K., and Momoi, T. (2006). Oligo-astheno-teratozoospermia in mice lacking RA175/TSLC1/SynCAM/IGSF4A, a cell adhesion molecule in the immunoglobulin superfamily. Mol Cell Biol *26*, 718-726.

Gray, E.G. (1959). Axo-somatic and axo-dendritic synapses of the cerebral cortex: an electron microscope study. J Anat *93*, 420-433.

Gresack, J.E., and Frick, K.M. (2004). Environmental enrichment reduces the mnemonic and neural benefits of estrogen. Neuroscience *128*, 459-471.

Jones, D.H., and Matus, A.I. (1974). Isolation of synaptic plasma membrane from brain by combined flotation-sedimentation density gradient centrifugation. Biochim Biophys Acta *356*, 276-287.

Knott, G.W., Holtmaat, A., Wilbrecht, L., Welker, E., and Svoboda, K. (2006). Spine growth precedes synapse formation in the adult neocortex in vivo. Nat Neurosci *9*, 1117-1124.

Li, C., Brake, W.G., Romeo, R.D., Dunlop, J.C., Gordon, M., Buzescu, R., Magarinos, A.M., Allen, P.B., Greengard, P., Luine, V., and McEwen, B.S. (2004). Estrogen alters hippocampal dendritic spine shape and enhances synaptic protein immunoreactivity and spatial memory in female mice. Proc Natl Acad Sci U S A *101*, 2185-2190.

Lister, R.G. (1987). The use of a plus-maze to measure anxiety in the mouse. Psychopharmacology (Berl) *92*, 180-185.

Mayford, M., Bach, M.E., Huang, Y.Y., Wang, L., Hawkins, R.D., and Kandel, E.R. (1996). Control of memory formation through regulated expression of a CaMKII transgene. Science *274*, 1678-1683.

Rabenstein, R.L., Addy, N.A., Caldarone, B.J., Asaka, Y., Gruenbaum, L.M., Peters, L.L., Gilligan, D.M., Fitzsimonds, R.M., and Picciotto, M.R. (2005). Impaired synaptic plasticity and learning in mice lacking beta-adducin, an actin-regulating protein. J Neurosci *25*, 2138-2145.

Rosahl, T.W., Spillane, D., Missler, M., Herz, J., Selig, D.K., Wolff, J.R., Hammer, R.E., Malenka, R.C., and Südhof, T.C. (1995). Essential functions of synapsins I and II in synaptic vesicle regulation. Nature *375*, 488-493.

Thomas, L.A., Akins, M.R., and Biederer, T. (2008). Expression and adhesion profiles of SynCAM molecules indicate distinct neuronal functions. J Comp Neurol *510*, 47-67.